01

Asymptotically spin forbidden quasimolecular radiative transitions (review)

© A.Z. Devdariani[1,2]

[1] St. Petersburg State University, St. Petersburg, Russia
[2] Herzen Russian State Pedagogical University,
191186 St.-Petersburg, Russia

e-mail: a.devdariani@spbu.ru

Received on August 04, 2021
Revised on August 04, 2021
Accepted on August 10, 2021

Theoretical works on radiative transitions produced in thermal collisions of atoms of groups 2A, 12 of the periodic table with atoms of inert gases in the normal state as well as in nonsymmetrical collisions of inert gas atoms are discussed in the review. Such collisions are accompanied by either the decay or the population of the lower metastable state $^3P_2$. The discussion has been carried out within the framework of analytical approaches based on the Fermi pseudopotential method and semiempirical method. The results on rate constants, absorption coefficients, radiative lifetimes, spectral profiles have been presented

Keywords: optical collision spectroscopy, quasimolecular state interaction, Fermi pseudopotential, semi empirical procedure of term reconstruction.

DOI: 10.21883/EOS.2022.14.53990.2609-21

Introduction. Quasimolecular radiative transitions. Forbidden transitions. Spin-forbidden transitions

The review relates to a theoretical description of the spectroscopy of single-quantum radiative transitions in diatomic quasimolecules, i. e., absorption/emission spectra, which are formed during slow pair collisions of atoms. The term „asymptotic forbidden" means, as in atomic spectroscopy, that the dipole moment of such transition becomes zero, but at large interatomic distances. At first thought, it might seen that there is no special need to pay attention to some special case of the relatively long and well-developed physics of broadening and shift of spectral lines, which deals precisely with the collisions effect on the shape of lines. For example, in the extensive review [1] known to spectroscopists, maximum one page is devoted to such transitions, which are called „forbidden"there. Already simple qualitative considerations, however, point to a significant difference between quasimolecular transitions, which are allowed or forbidden in isolated atoms.

Allowed transitions can be understood and described, at least approximately, as radiative transitions between two quasimolecular states that do not interact with other states. In the first approximation, we can assume that the central part of the contour of the allowed quasimolecular transition — Lorentz is located by frequency near the corresponding atomic transition. The broadening of the contour is associated with the long-range part of the interatomic interaction potential, and the satellites in the far wings are due to possible extrema in the difference between the potential curves of the initial and final states.

A satisfactory description of forbidden transitions in isolated atoms is made on the basis of high orders of perturbation theory [2] and leads to a significantly lower transition probability compared to allowed transitions. But the situation changes radically in the presence of buffer gas atoms. The interaction of an excited atom with a buffer gas atom is accompanied by a decrease in the symmetry of the electronic potential compared to an isolated atom, so that radiative transitions forbidden by parity, momentum, or spin in isolated atoms are allowed in quasimolecules.

The quasimolecular mechanism of the prohibition removal can be understood and described, as a rule, already in the first order of the perturbation theory, but for several states interacting with the initial excited state in the region of average interatomic distances $R \sim 10a_0$. The variety of mechanisms of interaction of atoms leads to the fact that the formed bands differ from the Lorentz ones and can no longer be described by a single formula. Another consequence of the need to take into account the interaction of excited states is that the description of forbidden radiative transitions turns out to be related to the problem of nonadiabatic transitions in collisions, so that there is an opportunity to extract information about nonadiabatic transitions in collisions of atoms from data on the shape of the contour [3]. Usually, at the first stage of the analysis of forbidden transitions, „a quantum-chemical (or static) problem"is solved in a certain sense, i.e., the dependence of the energy terms and dipole moments of the quasimolecule on the interatomic distance is determined in one way or another, and only then the problem of determining the shape of the spectrum of the corresponding transition is solved.

In this paper, we discuss the results of calculations and, in some cases, compare them with experimental data for transitions that are spin-forbidden in the *LS*-bond approximation in isolated atoms. The prohibitions removal relating the orbital momentum, especially for the quasimolecules of alkali metal atom–inert gas atom, has been developed in sufficient details [3–5]. In the review paper on the collisions effect on atomic spectral lines [1] only $s-s$, $s-d$ transitions in alkali metals are discussed. In the collective monograph [6] maximum one paragraph is devoted to forbidden quasimolecular transitions.

Note two more thematic features of the proposed review. It discusses quasimolecules of two types, composed of atoms of groups 2A, 12 of the Periodic Table with an excited two-electron configuration $nsnp$ and atoms of inert gases in the ground states, as well as asymmetric quasimolecules composed of excited atoms of inert gases with electron-hole configuration $np^5n's$, and inert gas atoms in ground states.

This choice of objects was made for two reasons. In both cases, we are talking, in essence, about the description of a two-particle excited configuration, which makes it possible to most clearly trace the mechanisms for the prohibitions removal on radiative spin transitions. On the other hand, the absence of symmetry in rearrangement of atoms makes it possible to significantly simplify calculations and restrict oneself to a transparent analytical approach for estimating the interaction in the region of average interatomic distances, which is responsible for removal of the prohibition on the radiative transition in the quasimolecule.

Radiation processes in symmetric quasimolecules represent a separate and important field, especially since one of the first papers on the theory of forbidden transitions was carried out by Allison et al. [7] on the calculation of the cross section of radiation induced by $\mathrm{He}(2^1S) + \mathrm{He}(1^1S)$ collisions. For the static part of the problem in [7] an analogue of LCAO was used. Radiation processes in symmetric collisions can also include processes involving ions, such as charge exchange. In particular, resonant charge exchange to the ground state of ion is accompanied by a quasimolecular radiative transition, the probability of which goes to zero at large distances R [8,9].

On the topic of forbidden transitions in the experiment. For obvious reasons, its „popularity“ is significantly below the popularity of the study of quasimolecular radiative transitions associated with allowed atomic transitions. See review [10] about those for the $nsnp$ configuration. Nevertheless, the discussed transitions are also interesting for experiment for at least two reasons. First, their study, as compared with atomic ones, is facilitated by a significantly higher transition probability, since it is due to the interaction of several quasimolecular states already in the first order. In addition, there is no need to extrapolate the data to zero density of the buffer gas. Secondly, the change in the concentration of atoms in metastable states, which often determines the properties of low-temperature plasma, is largely due to radiative transitions, which is especially true for quasimolecules containing a heavy atom. Note that the use of experimental data below is mainly illustrative and does not pretend to be complete.

Below, unless otherwise noted, atomic units are used.

1. Radiative transitions $nsnp\ {}^3P_2 \leftrightarrow ns^2\,{}^1S_0$

1.1. Mechanism of prohibition removal

The first discussion of the prohibition removal for the spin-forbidden radiative transition induced by thermal collisions of atoms of the 12 group of the periodic table (or, in the old terminology, the side subgroup of the II group)

$$M(nsnp^3P_2) + X(^1S_0) \to M(ns^2\,^1S_0) + X(^1S_0) + \hbar\omega, \quad (1)$$

where $M =$ Zn, Cd, Hg with heavy rare atoms $X =$ Ar, Kr, Xe was carried out in [11]. The discussion was based on the calculation of the matrix elements of the quasimolecule Hamiltonian:

$$\widehat{H} = \widehat{H}_{M^*} + \widehat{H}_X + \widehat{V}_{S0} + \widehat{V}, \quad (2)$$

in the basis of molecular functions composed of the products of the corresponding atomic functions in c basis according to Hund:

$$|^{1,3}P_j\Omega = 1\rangle = |M(^{1,3}P_j m_J)|X(^1S_0)\rangle, \quad (3)$$

$$j = 1, 2, 3, \quad m_j = 1.$$

For one excited configuration the matrix elements are expressed in terms of the Slater exchange integral G, the Lande coefficient, and the interaction potentials of $H_{\Sigma,\Pi}$ atoms in the states Σ and Π without taking into account the electrostatic and spin -orbital splitting of atomic levels $M(nsnp)$. In [11] these potentials were estimated within the framework of the asymptotic theory [12,13]. The prohibition removal for the radiative transition is caused by the interaction of three states. In the course of collisions with inert gas atom, the interaction of the excited states $^3P_1$, $^3P_2$ leads to splitting of Σ- and Π-terms: $\Delta H(R) = {}^3H_\Sigma(R) - {}^3H_\Pi(R)$, so the adiabatic quasimolecular wave function of the state $\Omega = 1\,^3P_2$ will include the wave function of the resonance state $^1P_1$, which, in its turn, is connected by spin-orbit interaction with the state function $^3P_1$ already in an isolated atom. Thus, the quasistatic radiation width of the quasimolecular state turns out to be proportional to the probability of a spontaneous resonant transition $^1P_1 \to {}^1S_0$. The shape of the spectrum averaged over the Maxwellian distribution of atoms with temperature T can be described in the first approximation as

$$W(\Delta\omega) = \frac{\Delta\omega}{T^2}\exp\left(-\frac{\Delta\omega}{T}\right), \quad (4)$$

where the frequency $\Delta\omega > 0$ is measured from the transition energy $^3P_2 \to {}^1S_0$. The radiation maxima form

transitions in the vicinity of the turning point for the classical motion of atoms in the potential $\Omega = 1$ ($^3P_2$). The total average cross section of radiation quenching turns out to be proportional to T^n, $n \approx 1.5-2.5$. Such a dependence on temperature agrees with experimental data, but the absolute value of the cross section for a number of pairs is by an order of magnitude smaller, although it significantly exceeds estimates based on perturbation theory as applied to the isolated atom. On the whole, the results [11] led to the conclusion that, when considering forbidden transitions in an atmosphere of buffer gases, the quasimolecular mechanism should be involved, but in order to achieve quantitative agreement with experiment, the theoretical approach should be more accurate and take into account the effect of nonadiabatic transitions and the associated violation of the quasistatic approximation for the shape of the spectral lines.

1.2. Calculation of interaction potential and radiation width

Focusing on the most important area of application for the processes under consideration i.e. low-temperature plasma, we can assume that the collision energies of atoms forming quasimolecules are thermal, therefore, for quantitative estimates, information is needed on the interaction potentials at medium and large interatomic distances. To analytically estimate the potentials in this region, one can use the method of the effective Hamiltonian [12]. With the use of this approach in [14–17] the potentials of the lower excited states of various asymmetric quasimolecules with atoms of the 12 group and inert gases were constructed. In this approach, the Hamiltonian is constructed as the sum of the Hamiltonians of the interacting excited atom with the buffer gas atom without taking into account the spin-orbit interaction:

$$\widehat{H} = \widehat{H}_{M*X} + \widehat{V}_{S0}. \tag{5}$$

As follows from Section 1.1, in order to calculate the radiative decay of a metastable atomic state $^3P_2$, it is necessary to take into account the interaction between quasimolecular states with the projection of the total momentum onto the molecular axis $\Omega = 1$. Bearing in mind the subsequent calculation of the radiation width, it is convenient to carry out such calculation in the basis of the wave functions that is intermediate between the a and c coupling types according to Hund. Indeed, at medium interatomic distances, the interaction of the orbital momentum with the axis prevails, while at large distances this interaction is comparable to and is smaller than the spin-orbit interaction in the excited atom. Functions of the intermediate type of coupling are built in two stages. At the first stage, among the distance-dependent functions $|R, (LS)\Lambda\Sigma\rangle^{(a)}$ in the Hund basis a, which diagonalize the Hamiltonian $\widehat{H}_{M^*X}$:

$$\langle R, (LS)\Lambda'\Sigma'|\widehat{H}_{M^*H}|R, (LS)\Lambda\Sigma\rangle^{(a)} = {}^{2S+1}H_{|\Lambda|}(R)\delta_{\Lambda\Lambda'}\delta_{\Sigma\Sigma'}, \tag{6}$$

functions of the diabatic basis are constructed for the case c:

$$|R, (LS)j\Omega\rangle^{(c)} = \sum_{\Lambda,\Sigma}\langle LSj\Omega|L\Lambda S\Sigma\rangle|R, (LS)\Lambda\Sigma\rangle^{(a)}, \tag{7}$$

$\langle LSj\Omega/L\Lambda S\Sigma\rangle$ — Clebsch-Gordon coefficients. In the case under consideration $j = 1, 2$, $\Omega = 1$, so that

$$|R, (10)11\rangle^c = |R, (10)10\rangle^a (= |^1\Pi_1\rangle), \tag{8}$$

$$|R, (11)21\rangle^c = \frac{1}{\sqrt{2}}\Big[|R, (11)10\rangle^a + |R, (11)01\rangle^a\Big] = \frac{1}{\sqrt{2}}(|^3\Pi_1\rangle + |^3\Sigma_1\rangle), \tag{9}$$

$$|R, (11)11\rangle^c = \frac{1}{\sqrt{2}}\Big[|R, (11)10\rangle^a - |R, (11)01\rangle^a\Big] = \frac{1}{\sqrt{2}}(|^3\Pi_1\rangle - |^3\Sigma_1\rangle). \tag{10}$$

In parentheses the more familiar notations for functions of the Hund case a are given. As can be seen from formulas (8), (10), the diabatic basis functions with $j = 1, 2$, $\Omega = 1$, but different spin values do not diagonalize the spin-orbit interaction operator, although for atoms Zn, Cd, Hg such interaction is essential. Therefore, at the second stage, when constructing wave functions of intermediate type of coupling, one should go to linear combinations:

$$|R, j\Omega\rangle^S = a|R, (10)j\Omega\rangle^{(c)}_{LS} + b|R, (11)j\Omega\rangle^{(c)}_{LS} = \varphi_1,$$
$$|R, j\Omega\rangle^T = -b|R, (10)j\Omega\rangle^{(c)}_{LS} + a|R, (11)j\Omega\rangle^{(c)}_{LS} = \varphi_3, \tag{11}$$

which, for large R diagonalize the Hamiltonian of excited atom with two electrons outside the filled shells (superscripts S, T indicate the dominant value of the spin). The amplitudes of the intermediate type of coupling a, b can be expressed approximately in terms of the spin-orbit interaction constant and the Coulomb exchange integral [18], assuming that they depend weakly on the distance, or can be determined from experimental data on levels splitting or transition probabilities in atoms [19]. The third function φ_2 c $\Omega = 1$ is the same as c (9). Table 1 lists the matrix elements in the basis of the functions $\varphi_i(\Omega = 1)$, $E_1 = E(^1P_1)$, $E_2 = E(^3P_2)$, $E_3 = E(^3P_1)$ are atomic energy levels of configuration sp,

$${}^{1,3}H_\Pi(R) = \langle {}^{1,3}\Pi_1|\widehat{H}_{M^*X}|{}^{1,3}\Pi_1\rangle,$$
$${}^3H_\Sigma(R) = \langle {}^3\Sigma_1|\widehat{H}_{M^*X}|{}^3\Sigma_1\rangle$$

are molecular terms defined in (10) for the case a without spin-orbit interaction, $\bar{H}(R) = [{}^3H_\Sigma(R) + {}^3H_\Pi(R)]/2$. Due

Table 1. Matrix elements $H_{ij}^{\Omega=1}$ in the basis of coupling type functions c for $\Omega = 1$ [17]

Basis	φ_1	φ_2	φ_3
H_{ij}	$E_1 + a^2 {}^1H_p(R) + b^2\bar{H}(R)$	$-(b/2)\Delta H(R)$	$ab[\bar{H}(R) - {}^1H_p(R)]$
	$-(b/2)\Delta H(R)$	$E_2 + \bar{H}(R)$	$-(a/2)\Delta H(R)$
	$ab[\bar{H}(R) - {}^1H_p(R)]$	$-(a/2)\Delta H(R)$	$E_3 + b^2 {}^1H_p(R) + a^2\bar{H}(R)$

to the low ${}^1H_\Pi$ in estimates we can assume that ${}^1H_\Pi = {}^3H_\Pi$ in matrix elements $H_{13,33}$.

Diagonalization allows one to define quasimolecular terms and adiabatic functions as linear combinations of functions (8)–(11):

$$|c, \Omega = 1\rangle^{ad} = \sum_{k=1}^{3} c_k(R)\varphi_k. \quad (12)$$

To calculate the radiation characteristics, it is convenient to return to the basis of the diabatic c-functions (8), (11):

$$|c, \Omega = 1\rangle^{ad} = (c_1 a - c_3 b)|R; (10)11\rangle_{LS}^{(c)} + c_2|R; (11)21\rangle_{LS}^{(c)} + (c_1 b + c_3 a)|R; (11)11\rangle_{LS}^{(c)}. \quad (13)$$

Since only the singlet state $|R; (1q0)111\rangle_{LS}^{(c)}$ is associated with the ground quasimolecular state $X^1\Sigma^+$ by the allowed dipole transition, then the dipole moment $d(R)$ of the radiative transition $c-X$ is

$$d(R) = [c_1(R)a - c_3(R)b]\langle X^1\Sigma^+|\widehat{D}|R; (10)11\rangle_{LS}^{(c)}, \quad (14)$$

while the probability of a quasimolecular radiative transition

$$\Gamma_{c-X}(R) = \left(\frac{a}{b}c_1(R) - c_3(R)\right)^2 \left(\frac{\omega(R)}{\omega({}^3P_1)}\right)^3 \Gamma({}^3P_1), \quad (15)$$

where $\omega(R), \omega({}^3P_1)$ are the frequencies of quasimolecular and atomic transitions, $\Gamma({}^3P_1)$ is probability of atomic transition.

Thus, to calculate the quasimolecular terms and the probabilities of spin-forbidden radiative transitions information on the matrix elements ${}^{1,3}H_{\Sigma,\Pi}$ is required. In the spirit of the effective Hamiltonian method, we can assume that these terms are the matrix elements of the operator of the interaction of atom M^* with an atom X without taking into account the spin-orbit interaction. Further, the calculations can be continued in two ways, either analytically, for example, using the asymptotic theory [12,13] in combination with well-founded models to describe the interaction of excited electron with a structureless atom X, or using a semi-empirical procedure involving the use of experimental data on the spectra of allowed quasimolecular transitions. Both approaches will be described and implemented below.

Note that, apparently, the first determination from experimental data of the potential curves of states involved in the asymptotically forbidden quasimolecular transition was undertaken in [20], and the first calculation of the corresponding terms in the quasirelativistic approach *ab initio* is in [21]. The mechanism for the prohibition removal and determining the dependence of the radiative transition probability were not considered in these papers.

1.3. Quasimolecules with light atoms of inert gases. Fermi pseudopotential

The main difficulty in applying the effective Hamiltonian method introduced for the problems under consideration in Section 1.2 is associated with estimating the matrix elements of the atoms interaction operator. To overcome it, two approaches were proposed and implemented. One of them is based on the use of the Fermi pseudopotential, the original form of which considered only the short-range part of the exchange interaction [22].

In the framework of the effective Hamiltonian method, the operator of interaction of colliding atoms $\widehat{H}_{M^*X}$ without spin-orbit interaction consideration is composed as the sum of the Hamiltonians of free atoms:

$$\widehat{H}_{M^*X} = \widehat{H}_{M^*} + \widehat{H}_X + {}^{2S+1}\widehat{H}_\Lambda \quad (16)$$

and the interaction ${}^{2S+1}\widehat{H}_\Lambda$, which is the sum:

$${}^{2S+1}\widehat{H}_\Lambda = \widehat{U} + \widehat{V}_{ion} \quad (17)$$

the effective one-electron operator of interatomic interaction $\widehat{U}$ and the operator $\widehat{V}_{ion}$ of the interaction of the ion core with buffer gas atom [23]. In the region of large and medium interatomic distances, for the last operator, we can limit ourselves to the approximate expression

$$V_{ion} = -\frac{\beta}{2R^4}, \quad (18)$$

where β is the dipole polarizability of the atom X.

To calculate the matrix elements of the operator of interatomic interaction in the case of light inert gases, one can use the Fermi pseudopotential [22], which depends on one parameter L i.e. the scattering length of excited electron on buffer gas atom:

$$\widehat{U} = 2\pi L\delta(\mathbf{r}) + \widehat{V}'.$$

The operator $\widehat{U}$ represents the sum of two terms — short-range exchange and polarization terms, taking into account the screening of the interaction of the ion core M^+ with the atom X by the field of the excited electron np [24]. The matrix elements of the short-range interaction of an

excited electron with a perturbing atom and the long-range polarization interaction, considering the interaction of three particles (M^+, e and X), were made in papers [25–27]. Diagonal elements for $\Lambda = \Sigma, \Pi$ are given in [14] for singlet and triplet states:

$$^{2S+1}I_\Sigma(R) = {}^{2S+1}U^{\text{ex}}_{p\Sigma} + {}^{2S+1}U^{scr}_{p\Sigma}, \;\; {}^{2S+1}H_\Pi(R) = {}^{2S+!}U^{scr}_{p\Pi}. \tag{19}$$

Here,

$$^{2S+1}U^{ex}_{p\Sigma} = 2\pi^{2S+1}B|Y_{10}(\mathbf{R}/R)|^2|^{2S+1}f_{np}(R)|^2 \tag{20}$$

is exchange interaction potential, $^{2S+1}f(\rho)$ are radial wave functions of excited electron np (as such in [14], for example, the atomic wave functions of the approximation of the effective orbital quantum number [28]) are used. The electron scattering length L is somewhat modified depending on the range of interatomic distances, so that

$$^{2S+1}B = L, \;\; \text{at } R < |1/^{2S+1}E^*|. \tag{21}$$

The expression for $U^{scr}_{p\Sigma\Pi}$ is given in [18].

1.4. Quasimolecules M^*-He, Ne. Quenching rate constant

The reason for the isolation of quasimolecules composed of atom with two valence electrons and atom of a light inert gas is clear from the discussion in Section 1.3. For such quasimolecules the terms and radiation widths can be calculated analytically using the known characteristics of free atoms, in particular, the scattering length. For heavy inert gases $X =$ Ar, Kr, Xe, such approach is unacceptable, since the significant polarizability violates the applicability conditions for the Fermi pseudopotential [25]. Another limitation, but already related to the excited atom, forces us to limit ourselves in this section to $M =$ Cd, Ba, Yb, Hg. The reason is that for light atoms, the distance between the levels $^3P_{1,2}$ involved in the process turns out to be comparable with the thermal energy of the collision, so that nondiabatic transitions must also be taken into account when analyzing radiative processes (for more details, see Section 1.8). Considering these limitations it is reasonable to start the discussion with Hg^*-He quasimolecule, especially since the small potential energy wells in the ground and excited states make it difficult to use laser-induced fluorescence methods. Just these methods were used to obtain the most reliable data on the characteristics of radiating states, which are necessary in the case of heavy inert gases (see Section 1.5 below). In the case of Hg^*-He, the experimental spectroscopic characteristics were obtained only for the state $0^+(^3P_1)$ [29]. The results of theoretical studies based on the considerations presented in Sections 1.2, 1.3 have already been presented in review papers [30,31], so only some new results are discussed below [32].

There are two related questions to the approaches of Sections 1.2, 1.3 i.e. just how the one-configuration approximation used is justified, and whether it is possible to represent the interaction of the ionic shell with a neutral atom by a simple polarization potential (18). The answers to these questions make it possible to refine the regions of interatomic distances, for which, nevertheless, it is possible to apply a simplified approach.

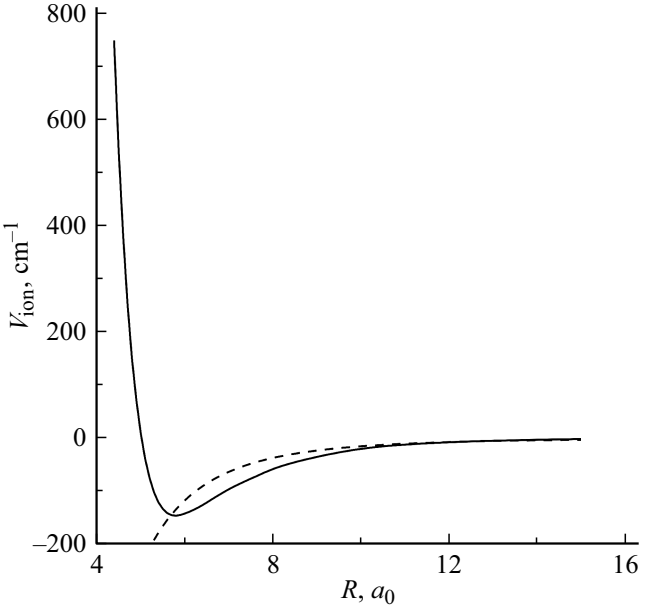

Figure 1. Potential curve of ion-atom interaction of Hg^+-He. Solid curve is result of ab-initio calculation V_{ion}, dashed curve is polarization interaction $V_{\text{ion}-p} = -\beta/2R^4$.

To study the effect of interconfigurational interaction, it is advisable to use the analytical expressions for the matrix elements of the interaction obtained in [26,33,34]. For the first time, such approach to studying the effect of interconfigurational interaction was applied in [35] for the Li^*-He quasimolecule. Comparison with multiconfiguration calculations *ab initio* [35] showed good agreement between the results, which made it possible to transfer the approach [34], which combines analytical estimates of the interaction and allowance for multiconfigurational interaction, and to the Hg quasimolecule $^*-$He.

In this approach, it was shown in [23] that for the states $^{1,3}\Pi$ the effect of the interaction with the nearest 13 excited configurations ns, d, f at $R \le 7a_0$ is not essential. For configurations $^{1,3}\Sigma$, the effect of interaction between configurations turns out to be more significant, but for thermal collisions such interaction only slightly changes the position of the turning point on the classical trajectory in the region $R \sim (8-9)a_0$. On the whole, the results of multi-configuration calculations [34,35] allow us to conclude that even a single-configuration approximation gives satisfactory results at binding energies of the electron in atom below 5 eV, and is justified for atoms with low polarizability, i. e. for He, Ne. Less encouraging results were obtained in [31] to describe the interaction of the ionic core with buffer gas atom V_{ion}. The use of a simple formula (18) in the case of $X =$ He is justified only for $R \ge 7a_0$, where

Table 2. Interaction potential parameters for $Hg(6^{1,3}P_J) + He$

State	R_e, a_0			D_e, cm^{-1}		
Calculation options	*a*	*b*	*c*	*a*	*b*	*c*
$0^-(^3P_0)$	8.7	10.0	12	13	3.0	1.6
$0^+(^3P_1)^d$	6.2	–	11.5	58	–	1.9
$1(^3P_1)$	9.1	10.4	12.3	10.4	3.1	1.3
$2(^3P_2)$	5.8	–	7.0	108	–	29
$1(^3P_2)$	9.1	10.5	12.4	10	3.0	1.1
$0^-(^3P_2)$	9.5	10.7	> 13.5	8	3.1	0.8
$1(^1P_1)$	5.8	–	7.4	131	–	20
$0^+(^1P_1)$	14.0	14.4	> 14	1.3	1.3	–

Note. *a* is calculation results [32]; *b* are calculations [23] using the polarization approximation for the potential V_{ion}; *c* are calculations [34] using the potential from [42] for states $^{1,3}\Sigma$ and $^{1,3}\Pi$; *d* — for the state $0^+(^3P_1)$ experimental values R_e, D_e and D_0 are respectively $R_e = 6.54$ [43], 6.6 [44], $6.8a_0$ [45]; $D_e = 28\,cm^{-1}$ [43]; $D_0 = 28$ [44], 29 ± 2 [45], $13 \pm 2\,cm^{-1}$ [43].

the exchange repulsion of the Hg^+ ion and He atom is insignificant. In the region of smaller distances, one should use the ion-atom interaction potential, which is obtained by some independent method, for example, from experimental data or as a result of non-empirical calculation. This is how the potential of the ion-atom interaction Hg^+-He was obtained in [32] (Fig. 1) — using the multi-reference method of configuration interaction, taking into account single and double excitations (MRD-CI) [36–40] combined with the relativistic effective core potential (RECP) method [39–41]. As can be seen from Fig. 1, for $R < 5.5a_0$ the use of formula (18) is unacceptable. Correct consideration of the repulsive part of the ion-atomic potential made it possible to determine the terms in a wider range of distances (Fig 2) compared to [23], as well as the characteristics of the deepest potential energy wells of states $1(^1P_1)$, $2(^3P_2)$, $0^+(^3P_1)$ (Table 2, where the experimental data for states 0^+ are also presented). Note that the calculated value by two times exceeds the experimental value, while the calculation using matrix elements from paper [42] (for more details see Section 1.5) underestimates the value D_e by more than order of magnitude.

According to the term pattern (Fig. 2), due to the quasimolecular radiative transition $1(6^3P_2)-0^+(6^1S_0)$ the decay of the metastable state $Hg(6^3P_2)$ forms a band that is shifted to the short wavelength region with respect to the frequency of the forbidden atomic transition $\omega_2(6^3P_2-6^1S_0)$. The shift $\hbar\Delta\omega_m$ of the emission band maximum with respect to ω_2, as well as the distribution width are comparable to kT.

The radiation quenching rate constant is of practical interest:

$$K(T) = \frac{2}{5}4\pi \int_0^\infty \Gamma(R)\exp[-U(R)kT]R^2dR \qquad (22)$$

in the process

$$Hg(6s6p^3P_2) + He(^1S_0) \rightarrow Hg(6s^{21}S_0) + He(^1S_0) + \hbar\omega,$$

where Γ, U is the radiation width and interaction potential of the state $c1(^3P_2)$, 2/5 is a statistical factor. The results of the calculation of $K(T)$ in various approximations in the temperature range from 100 to 1000 K are given in Table 3. The constant increasing with temperature is associated with the distance decreasing of maximum approach of atoms and accompanying increase in the exchange interaction. Note that the interaction of configurations consideration has a weak effect on $K(T)$ value in comparison with the effect of the polarization ion-atom interaction [32,46].

Calculations for Yb, Ba, and Cd atoms were also performed in the one-configuration approximation (the inclusion of the lanthanide Yb is justified, since many Yb* levels can be considered in the two-electron approximation) [47]. As in the case of the mercury atom, quasimolecular radiation forms a narrow peak in the vicinity of the forbidden atomic transition $^3P_2-^1S_0$ 1000 cm^{-1} wide. The values of the corresponding rate constants are given in Table 4. The calculations were carried out according to formula (22), which, strictly speaking, is valid only for the repulsion potential $U(R)$, but in the case of $X = He, Ne$ the potential energy wells are

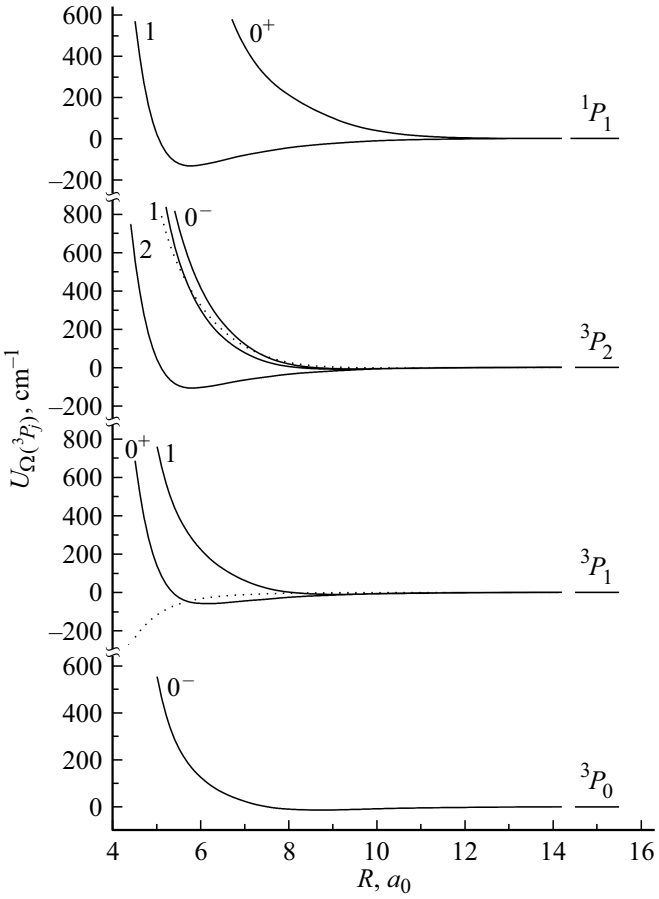

Figure 2. Interaction potentials of $Hg(6s6p)-He$. Solid curves — calculation [32], dashed curves – calculation [23] for states $1(^3P_2)$ and $0^+(^3P_1)$ taking into account only the polarization component of the ion-atom interaction.

Table 3. Rate constants K_{c-X} (in $10^{-18}\,\mathrm{cm^3 s^{-1}}$) of collisionally induced radiative decay $\mathrm{Hg}(6s6p^3P_2) + \mathrm{He}(^1S_0) \to \mathrm{Hg}(6s^{21}S_0) + \mathrm{He}(^1S_0) + \hbar\omega$

T, K	K_{c-X}		
Calculation options	*a*	*b*	*c*
100	0.41	0.26	0.26
200	1.0	0.87	0.82
300	1.8	1.7	1.6
400	2.6	2.8	2.6
500	3.5	4.0	3.8
600	4.4	5.2	5.1
700	5.3	6.5	6.4
800	6.2	7.9	7.8
900	7.1	9.3	9.2
1000	7.9	10.6	10.7

Note. *a* are calculation results [32]; *b* are calculations [15] taking into account the contribution of only the polarization interaction $V_{\mathrm{ion}-p}$ in multiconfiguration calculation of terms; *c* — taking into account the contribution of only the polarization interaction $V_{\mathrm{ion}-p}$ in one-configuration calculation of terms.

Table 4. Rate constants ($K \times 10^{18}$, $\mathrm{cm^3 s^{-1}}$) of collisionally induced radiative decay $M(^3P_2) + X(^1S_0) \to M(^1S_0) + X(^1S_0) + \hbar\omega$; M = Cd, Ba, Hg, Yb; X = He, Ar, Kr, Xe

T, K	*MX*						
	CdHe	BaHe	YbHe	HgNe*	HgAr*	HgKr*	HgXe*
100	0.07	0.24	0.29	0.33	1.8	5.0	13.4
200	0.20	0.62	0.89	0.86	2.9	6.6	15.5
300	0.36	1.00	1.61	1.5	4.3	8.5**	18.5***
400	0.53	1.37	2.40	2.3	5.7	10.5	20.5
500	0.68	1.74	3.25	3.1	7.2	12.5	23.0
600	0.87	2.12	4.12	4.0	8.6	14.6	25.9
700	1.05	2.50	5.15	4.9	10.3	16.7	28.7
800	1.22	2.90	6.27	5.9	11.9	18.8	31.5
900	1.39	3.20	7.55	8.1	13.5	21.0	34.4
1000	1.55	3.86	9.04	7.9	15.1	23.2	37.3

Note. * are calculations [46]; ** are experimental values (in units of $10^{-18}\,\mathrm{cm^3 s^{-1}}$) at $T = 305, 346$ and 373 K are 6.1, 6.9 and 7.5 [9] respectively; *** are experimental values (in units of $10^{-18}\,\mathrm{cm^3 s^{-1}}$) at $T = 303, 330$ and 385 K are respectively 130 ± 22, 140 ± 30 and 170 ± 20 [48] and $K(293\,\mathrm{K}) = 16$ [49].

$D_e \ll kT$, so the limitation associated with the centrifugal barrier can be neglected (for details see Section 2.5). A feature of the calculated values of $K(T)$ is that they are close to the corresponding values for the case of $\mathrm{Hg}^*-\mathrm{He}$. This is due to the fact that the decrease in the deviation from the *LS* bond compared to the Hg atom and the accompanying decrease in the probability of a radiative atomic transition $^3P_1 - {}^1S_0$ is compensated by a shift in the range of strong mixing of state functions $1(^3P_1, {}^3P_2)$ as $\Delta = E_2 - E_3$ decreases into the region of larger distances.

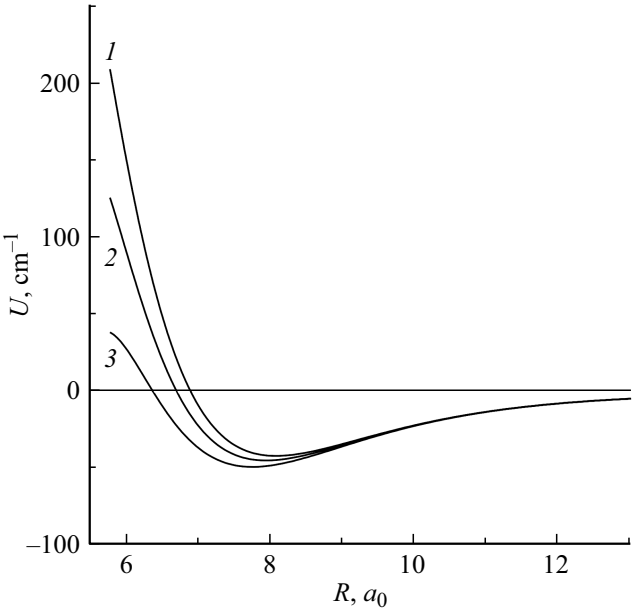

Figure 3. Interaction potentials $\mathrm{Hg}(6s6p)-\mathrm{H_2}$ at $\theta = 0$ (*1*), $\pi/4$ (*2*), $\pi/2$ (*3*).

The advantage of the above approach, which combines the effective Hamiltonian and pseudopotential methods, is that it can be relatively easily transferred to the case of molecular buffer gases, for example, $\mathrm{Hg}^*-\mathrm{H_2}$. The quadrupole interaction of excited electron with a molecule mixes states with different projections of the electron angular momentum on axis z, which connects the excited atom and the center of mass of the molecule $\mathrm{H_2}$, and leads to the energy of the states depending on the angle θ between axis z and the molecular axis. As an example, Fig. 3 shows the dependence of the interaction $\mathrm{Hg}(6^3P_0)-\mathrm{H_2}$ on R and θ [31]. This calculation did not consider the dependence of the exchange interaction of the ionic core with the hydrogen molecule on R and θ, so that the results are valid only in $R > 6a_0$ region; nevertheless, the approach used and the calculation can be used to analyze the wings of spectral lines generated by collisions with molecules.

1.5. Quasimolecules $M^* + $ Ar, Kr, Xe. Quenching rate constant

The strong polarization interaction of an excited electron with a heavy atom of inert gas prevents the use of the Fermi pseudopotential. Nevertheless, the approach proposed in Section 1.2, which is based on calculating the matrix elements of the effective Hamiltonian, makes it possible to obtain realistic estimates of the potentials and probabilities of radiative transitions of the involved quasimolecular states. The estimate is based on the fact that the distance dependences of all eight quasimolecular states generated by the $nsnp$ configuration can be expressed in terms of four functions $^{1,3}H_{\Sigma,\Pi}(R)$ are the interaction potentials in the Σ and Π states without spin-orbit splitting.

Table 5. Matrix elements $H_{ij}^{\Omega=1}$ in the basis of coupling type functions c for $\Omega = 0^+$ [17]

Basis	$\lvert R, D, 10^+\rangle^S$	$\lvert R, A, 10^+\rangle^T$
H_{ij}	$E_1 + a^{21}H_\Sigma(R) + b^{23}H_\Pi(R)$	$-ab\Delta H(R)$
	$-ab\Delta H(R)$	$E_3 + b^{21}H_\Sigma(R) + a^{23}H_\Pi(R)$

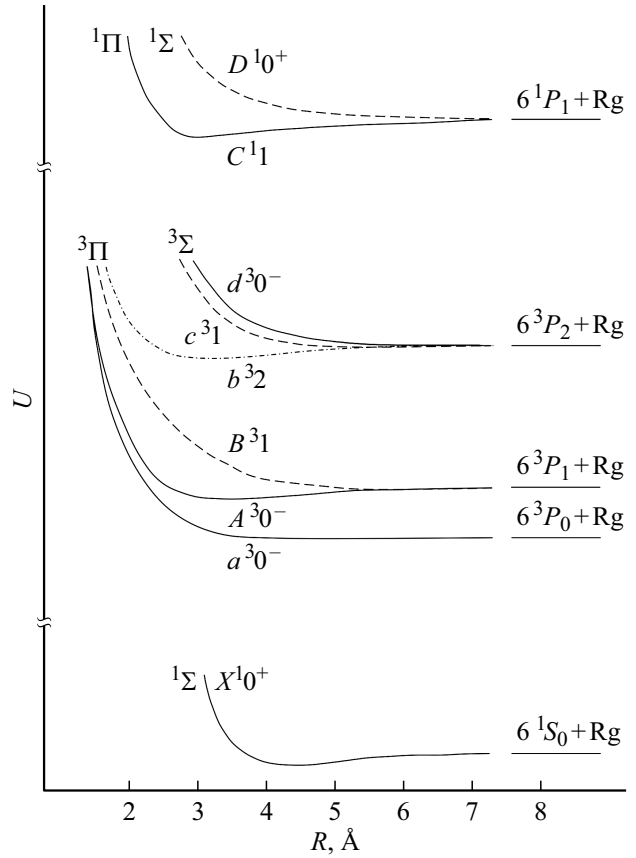

Figure 4. Schematic pattern of quasimolecular terms $M^*(nsnp)$ — Ar, Kr, Xe.

Indeed, matrix elements for states with $\Omega = 1$ (Table 1) were already used in Section 1.2, and for states with $\Omega = 0^+$ they are given in Table 5. The diagonalization of these matrices allows us to define, in particular, the terms A $0^+(^3P_1)$ and B $1(^3P_1)$ (Fig. 4), which are involved in the formation of the wings of the allowed transition $^3P_1 - {}^1S_0$, red and violet, respectively. Comparing the obtained terms with those that can be determined from the experimental data on the wings of the spectral line, it is possible to restore the dependences of the matrix elements $^{1,3}H_{\Sigma,\Pi}(R)$, if we assume that the singlet and triplet elements are the same. The estimate of the error of such a simplification in [16] showed that the replacement does not lead to a significant change in the potentials.

Table 6 compiled from the data [16,51] gives the characteristics of the potential state curves $1(^3P_2)$ for a number of quasimolecules recovered within the framework of the

Table 6. Characteristics of potential energy wells of the state with $\Omega = 1(^3P_2)$ quasimolecules Hg(6^3P_2) [16], Cd(6^3P_2) [51] — Ne, Ar, Kr, Xe

Quasimolecule	R_e, a_0	D_e, cm^{-1}	ω, cm^{-1}
Hg-Ne	9.34	13	8.0
Hg-Ar	9.00	51	12.5
	8.88*	61.1*	11**
		56**	
Hg-Kr	8.70	91	
	8.75*	103.3*	
Hg-Xe	8.83	180	12.5
Cd-Ar	9.48	57	12
Cd-Kr	9.25	108	11

Note. * — according to [17], ** — according to [50].

semi-empirical approach, as well as those obtained directly in the experiment [50]. The restored potentials are valid for $R > 7a_0$, and their common feature is the presence of the well capable of maintaining several vibrational states. Here it is appropriate to make one general remark about the semi-empirical method of terms determination. The point is that the terms $0^+(^3P_1)$, $1(^3P_1)$, determined from experimental data, are used in the form of Morse potentials for restoring the terms of configurations $nsnp$, strictly speaking, are valid in the vicinity of the minima of the radiating states. In the same region of interatomic distances, the restored terms should also be valid. Therefore, the distance dependence of the terms and the associated reliability of describing the distant wings of spectral lines formed by transitions far from the region of the minima of the radiating potentials cannot claim greater accuracy.

Since the diagonalization of the part of the Hamiltonian for the states $\Omega = 1$ (Table 1) also determines the coefficients c_i in formula (13), the described procedure for restoring the potentials allows us to determine the radiation width of the state c $1(^3P_2)$. It is convenient to introduce the dimensionless reduced radiation width

$$\gamma_{c-X}(R) = \frac{\Gamma_{c-X}(R)}{\Gamma(^3(P_1)}\left(\frac{\Omega(^3P_1)}{\Omega_{c-X}(R)}\right)^3, \qquad (23)$$

which does not depend on the ground state of the quasimolecule and characterizes the ratio of the squared dipole moment of the quasimolecule and the dipole moment of the atomic transition $^3P_1 - {}^1S_0$. As an example, Fig. 5 shows graphs of $\gamma(R)_{c-X}$ from the paper [52] of quasimolecules Hg*–He, Ne, Ar, Kr, Xe. The radiation width s are characterized by a strong distance dependence, as well as by vanishing in the vicinity of $R \sim 9-10a_0$. The latter circumstance is related to the fact that in the approximation used the dipole moment is proportional to $\Delta H = H_\Sigma - H_\Pi$, so at large R, where the long-range interaction prevails, $\Delta H < 0$, while for small R the exchange interaction prevails, and $\Delta H > 0$.

One remark before discussing the results on the rate constants of radiative quenching of the metastable state

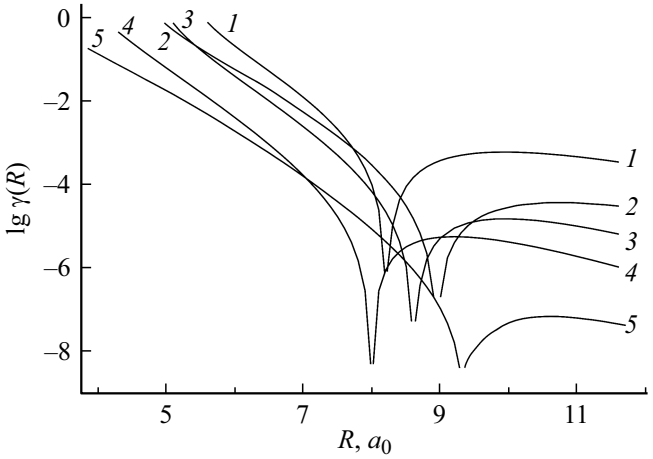

Figure 5. Reduced radiation width s $\gamma(c1(^3P_2))$ depending on R: Hg-Xe (*1*), Hg-Kr (*2*—*/*), Hg-Ar (*3*), Hg-Ne (*4*), Hg-He (*5*) [52].

Table 7. Rate constants K_{c-X} (in $10^{-17}\,\mathrm{cm^3 s^{-1}}$) of collisionally induced radiative decay of $Hg(6s6p^3P_2)$ in Ne, Ar, Kr, Xe

T, K	K_{c-X} (Ne)	K_{c-X} (Ar)	K_{c-X} (Kr)	K_{c-X} (Xe)
100	0.033	0.18	0.64	1.34
200	0.086	0.29	0.89	1.55
300	0.15	0.43	1.13	1.85
400	0.23	0.57	1.35	2.05
500	0.31	0.72	1.58	2.30
600	0.40	0.86	1.79	2.59
700	0.49	1.03	2.01	2.87
800	0.59	1.19	2.22	3.15
900	0.81	1.35	3.43	3.44
1000	0.79	1.51	2.65	3.73

$M^*(^3P_2)$. The existence of potential energy wells in the term $c1(^3P_2)$, comparable to kT, has already been noted above, which leads to a limitation of the range of impact parameters in the classical motion of atoms. This limitation should be taken into account when we discuss radiation induced by paired free-free and free-bound transitions during collisions, since transitions from bound states in the potential energy well of the excited state also partially contribute to this region [53–55]. Table 7 shows the results of calculating the quenching rate constants for Hg^*-Ne, Ar, Kr, Xe quasimolecules using formula (22), which takes into account both types of transitions from both free and coupled states. The paper [15] also presents the results of calculations of the quenching constant, which take into account transitions involving free atoms only. Taking into account the insignificant depth of the potential energy well kT, the results of calculations in two limiting cases coincide even for the pair Hg^*-Xe for $T > 500\,\mathrm{K}$. For $X =$ He, Ne, we can assume that the interaction is repulsive.

For quasimolecules with a Cd atom the condition, under which one can neglect nondiabatic transitions from the state $^3P_2$ to the nearest atomic radiant state $^3P_1$, is met somewhat worse than in the case of the Hg atom, the splitting is $1171\,\mathrm{cm^{-1}}$ versus $4631\,\mathrm{cm^{-1}}$ in the Hg atom. Potential curves and radiation width s for Cd−Ar, Kr quasimolecules calculated in the approach discussed above are given in papers [56,57]. As in the case of Hg, the potential curve $c1(^3P_2)$ is characterized by the presence of potential energy well at $R \sim 9a_0$ with depth $\sim 100\,\mathrm{cm^{-1}}$, and for the width — the presence of a root in the same range of distances.

Above, with the exception of the discussion of $Hg-H_2$ quasimolecule in Section 1.4, it was assumed that the buffer gas X is monatomic, structureless. The transition

Table 8. Probabilities $A(\nu', \nu'')$ (in $\mathrm{s^{-1}}$) of transitions $\nu'1(^3P_2) - \nu''0^+(^1S_0)$ in Hg-Ar, Kr, Xe quasimolecules

Rg	Ar					
ν''	ν'					
	0	1	2	3	4	5
0	88	277	500	673	–	–
1	409	900	1157	1143	–	–
2	555	635	365	123	–	–
3	197	23	41	171	–	–
4	0	38	97	51	–	–
5	17	2	0	26	–	–
Rg	Kr					
ν''	ν'					
	0	1	2	3	4	5
0	16	77	210	410	660	940
1	190	700	1470	2320	3040	3520
2	820	2140	3150	3400	3010	2290
3	1670	2460	1780	700	80	44
4	1560	670	0.1	433	1080	1290
5	540	44	730	770	280	4
Rg	Xe					
ν''	ν'					
	0	1	2	3	4	5
0	140	669	1765	3418	5545	7577
1	910	3090	5690	7520	7920	6970
2	2190	4500	4400	2410	530	23
3	2380	1950	190	440	2130	3240
4	1040	18	920	1850	1040	73

Table 9. Radiation times $\tau(\nu')$ of $\nu'c1(^3P_2)$ states of CdAr and CdKr [51,64] quasimolecules

ν'	$\tau(\nu')$, s	
	CdAr	CdKr
0	$3.7 \cdot 10^{-3}$	$1.3 \cdot 10^{-3}$
1	$1.6 \cdot 10^{-3}$	$6.2 \cdot 10^{-4}$
2	$1.2 \cdot 10^{-3}$	$4.3 \cdot 10^{-4}$

to diatomic molecules, even not considering the electronic excitation, complicates the analysis of quasimolecular optical transitions. Absorption in the far wing of the collision complex $Hg(^1S_0 \rightarrow {}^3P_2)-N_2, CO$ was measured for the first time in paper [57], which was accompanied not only by the predominant population of the state $Hg(^3P_2)$, but also by the population of $Hg(^3P_1)$ state, which, of course, is absent when the molecular buffer is replaced by inert gas. This result was explained in [57] by the excitation of the vibrational states of the N_2K, CO molecules, which makes it possible to reduce the energy defect between the initial and final states.

A few remarks at the end of this Section. The results presented were based on the development of a semi-empirical method for calculating terms and radiation widths. In essence, this approach continues the semi-empirical approach to the analysis of atomic terms described in [58], where terms of the same configuration are expressed in terms of several parameters, which, in turn, are determined by comparison with experimental data for radiating states. Another important point is construction of atomic wave functions of intermediate coupling type in the basis of *LS*-coupling functions, which could be called the basis of zero-order functions [15–17,59].

Pay attention to the fact that the dipole moment of the optical transition changes sign, i. e., changes orientation to the opposite, approximately at the boundary of the region of dominance of long-range or exchange forces. Here the situation also resembles the vanishing of the dipole moment known in the physics of the atomic photoelectric effect [60,61], but at a certain absorption frequency. The presence of zeros of the dipole moment depending on the distance between nuclei with charges $Z_{1,2}$ was also established in the exact calculation of the moments in the one-electron problem [62].

1.6. Lifetimes of vibrational states in the potential $c1(^3P_2)$

The calculation results presented in Section 1.5 predict the presence of potential energy wells $D_e \sim 100\,\text{cm}^{-1}$ at $R_e \sim 9a_0$ for Hg, Cd−Ar, Kr, Xe quasimolecules. In [50] the first direct experimental observation of a bound-bound transition $c-X$ is reported. The optical excitation of vibrational states in the $c1(^3P_2)$ potential for Hg−Ar was monitored by subsequent excitation to the overlying state E. The position of 7 vibrational levels was determined, which made it possible to plot the Birge-Sponer graphic and determine $D_e = 56\,\text{cm}^{-1}$ and $\omega_r = 11\,\text{cm}^{-1}$ (approximation by Morse potential) in accordance with the data of Table 6.

The next question, which is related to vibrational states and may be of interest for the physics of laser media, is the estimate of the probabilities of radiative transitions ν', which, according to Section 1.2, (17), is defined as

$$A(\nu', \nu'') = \frac{\omega(^3P_)2)}{\omega(^3P_1)}\Gamma(^3P_1)\left|\left\langle \nu' \left| \frac{ac_1}{b} - c_3 \right| \nu'' \right\rangle\right|^2, \quad (24)$$

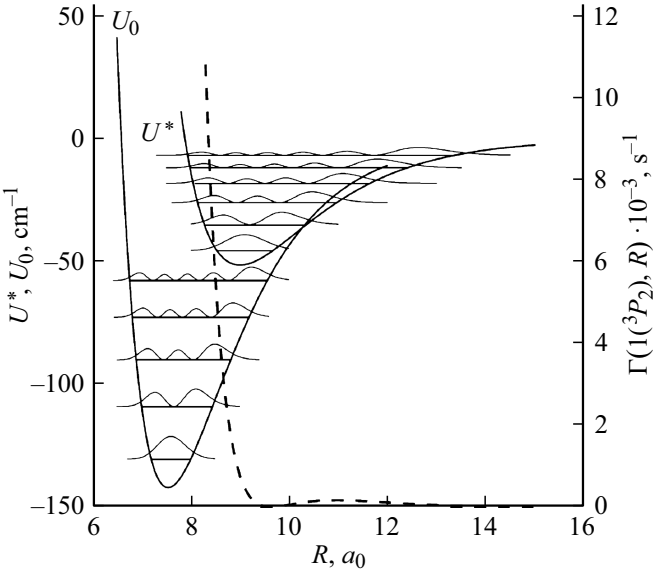

Figure 6. CdKr quasimolecule. Morse potentials for excited $U^*(c1(^3P_2))$, and ground U_0 states, positions of energy levels of vibrational states, and probability density distributions (solid lines), probability of quasimolecular radiative transitions (dashed line) [65].

where $|\nu', \nu''\rangle$ are wave functions of vibrational states in the excited term $c1(^3P_2)$ and the ground term $X(^1S_0)$, as well as an estimate of the state lifetime

$$\tau^{-1}(\nu') = \langle \nu' | \Gamma(1(^3P_2), R) | \nu' \rangle. \quad (25)$$

Both characteristics were calculated in paper [63] for the Hg−Rg quasimolecule and in [51,64] for Cd−Rg. In these papers, for the ground state potentials the data of papers [65] for Hg and [66] for Cd were used. As an example, Table 8 gives data on the transition probabilities for quasimolecules with Hg atom, and Table 9 — data on lifetimes for quasimolecules with Cd atom. It is appropriate to mention here that the lifetimes of atomic metastable states are equal to $\tau_m = 6.5\,\text{s}$ ($Hg(6^3P_2)$), 130 s ($Cd(5^3P_2)$) [67].

On the whole, the transition probabilities vary over a wide range, which is due to the effect of the strong dependence of the transition dipole moment on the interatomic distance and the degree of overlap of the vibrational functions of the initial and final states (Fig. 6) [64]. For the lower levels ($\nu' < 3$), the decrease in lifetime with ν' increasing is due to the abrupt increasing of the radiation width with decreasing of interatomic distance. A further increasing of vibrational excitation is accompanied by a decreasing of the functions overlap and shift of the transition to the region of medium distances, where the width now changes insignificantly, so that the upper vibrational states remain long-lived. Nevertheless, note that the interaction, for example, with the Kr atom reduces the lifetime of Hg, Cd−Kr excimer by 10^4-10^5 times as compared to the isolated atomic state $^3P_2$.

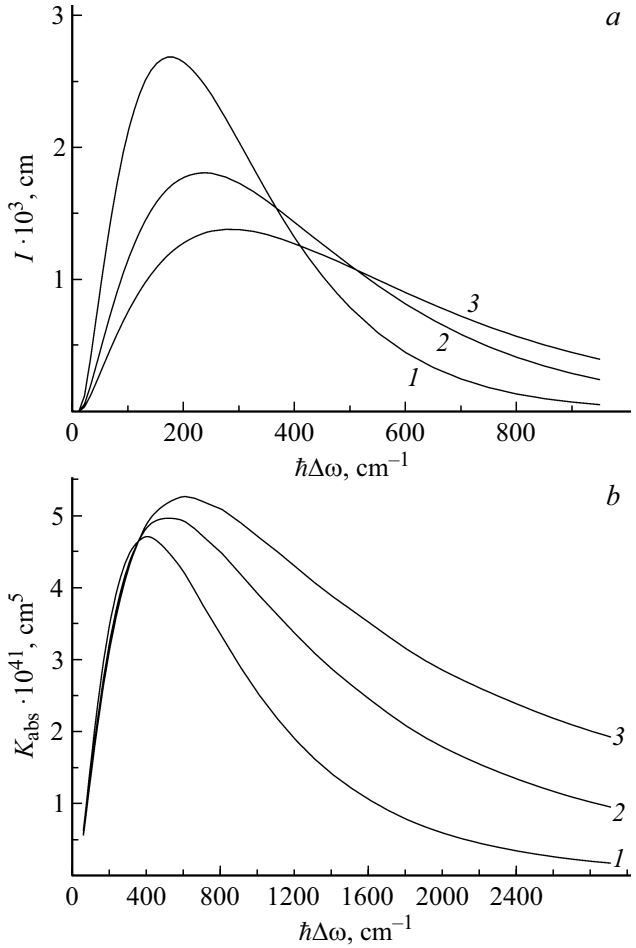

Figure 7. Normalized spectral distributions of quasimolecular radiation (*a*) and absorption (*b*) Hg(6^3P_2)–Ne [75]: $T = 300$ (*1*), 500 (*2*), 700 K (*3*).

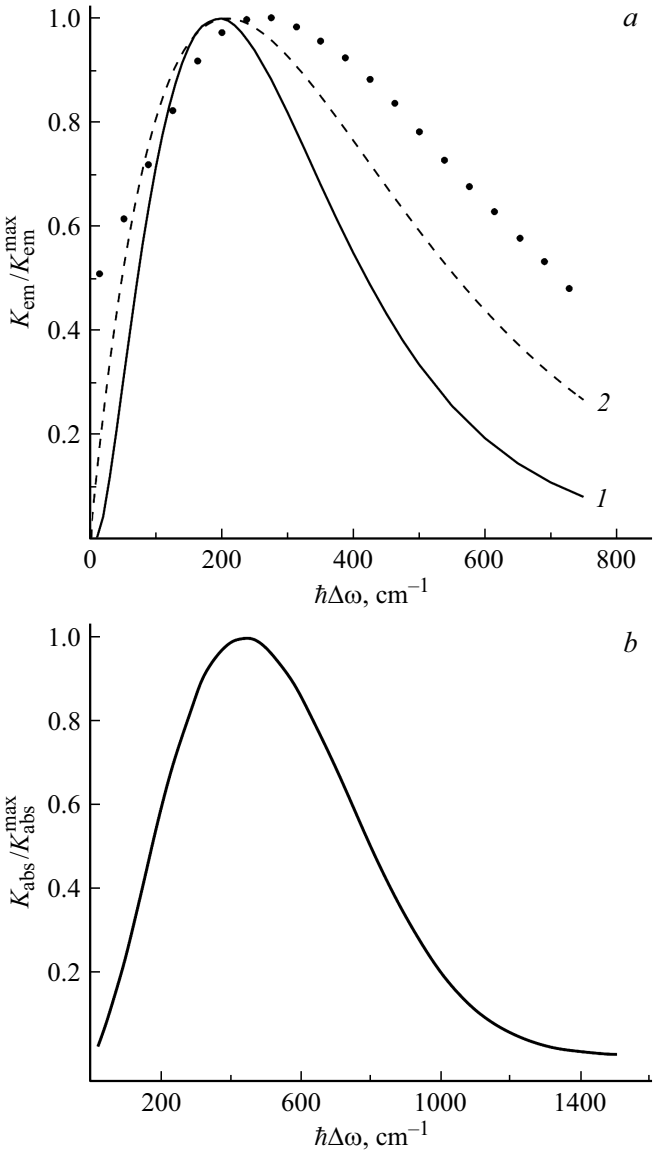

Figure 8. Quasimolecular radiative transitions Hg(6^3P_2)–Ar: (*a*) radiation at $T = 292$ K, referred to the maximum in the band, points — experiment [59], *1* — calculation [75], *2* — asymptotic estimate [4]; (*b*) absorption, also referred to the maximum [17], the experimental and calculated data coincide on the graph scale.

1.7. Spectrum of radiative transitions involving $c1(^3P_2)$ state in quasistatic approximation

The forms of the absorption/emission spectra for Hg, Cd–Ar, Kr, Xe quasimolecules are discussed below. For these pairs, the available experimental data on the shapes of the spectra of asymptotically allowed transitions make it possible, using a semi-empirical procedure, to reconstruct the potential state curve $c1(^3P_2)$ and the radiation width . Another feature of the chosen quasimolecules is the possibility of neglecting nonadiabatic transitions between states during thermal collisions, which at large R degenerate into atomic $^1P_1$, $\{3\}P_2$. In this case, the radiative transition can be described as transition between two states with energies $U_0 + \hbar\omega$ and $U^*(c1(^3P_2))$.

The fundamental basis of the quantum description of radiative processes in collisions of atoms under such conditions is provided mainly in the papers [68–71], for further development see [72]. In this approach, called the quasistatic theory, it is assumed that the radiative transition between two electronic states in a quasimolecule occurs in the vicinity of the Condon point R_c, which is determined by the condition that the photon energy and the difference potential are equal, i. e.

$$\Delta U(R = R_c) = U^* - U_0 = \hbar\omega. \qquad (26)$$

Using the semiclassical approximation for the trajectory of atoms allows us to write a simple formula for the shape of the spectrum. It turns out [73] that, as in the case of an isolated atom, it is sufficient to calculate the Fourier component of the matrix element of the dipole moment D, but which is now calculated on the time-dependent wave functions of the quasimolecule. For example, the amplitude

of photon emission has the form

$$b(\omega) = -i \int \sqrt{\frac{2(\alpha\omega^3)}{3\pi g}} D(t) \exp\left[-i \int [\Delta U - \omega] dt'\right] dt, \tag{27}$$

where the square of the pre-exponential factor is, up to 2π, the Einstein coefficient (or the radiation width Γ) for the radiation of the quasimolecule at time t, α is the fine structure constant. After summing over the impact parameters and averaging over the Maxwellian velocity distribution, formula (27) leads to the well-known expression for the spectral line wing in radiation in the quasi-static approximation:

$$K(\omega, T) = 4\pi R_c^2 \frac{\Gamma(R_c)}{|\frac{d}{dR}\Delta U(R_c)|} \exp\left[-\frac{U^*(R_c)}{kT}\right] \tag{28}$$

and to the absorption coefficient

$$\gamma(\omega, T) = \pi\lambda^2 R_c^2 \frac{\Gamma(R_c)}{|\frac{d}{dR}\Delta U(R_c)|} \exp\left[-\frac{U_0(R_c)}{kT}\right]. \tag{29}$$

The last two formulas, after multiplying (28) by 2/5, were used to calculate the short-wavelength wings of the spectra of $c-X$ quasimolecular transitions in collisions of Hg, Cd atoms with atoms of inert gases in the ground state [74,75]. In the calculation, we used the terms and radiation width s obtained using the pseudopotential method, Section 1.4, and also in the case of Ne, using the semi-empirical method. A detailed discussion of the terms and comparison of non-empirical results with semi-empirical results for these pairs is given in [14,32], and the results for emission and absorption contours for various gas cell temperatures in the case of Hg–Ne [75] are shown in Fig. 7. They are characterized by two features, which are due to the nature of the dependence of terms and radiation width on the interatomic distance. The absorption maximum is shifted to the short-wavelength region compared to radiation, since the repulsion of the excited electron by He, Ne atoms is observed at larger distances compared to the repulsion by a normal shell ns^2, so the transitions are concentrated in the region where the radiation width is small. For the same reason, there are no transitions in the long-wavelength region of the spectrum $\omega < \omega_0$ ($^3P_2 \leftrightarrow {}^1S_0$). Another feature is a noticeable absorption increasing with temperature rise, since this leads to the distance decreasing of closest approach of atoms and the transition probability increasing. The possible effect of transitions from bound and quasi-bound states is discussed below.

Let's now review transitions in the quasimolecules Hg–Rg, Rg = Ar, Kr, Xe. For the Ar case calculations for emission and absorption were made in [75], and the temperature dependence of the shape of the emission spectrum was calculated and compared with experimental data in [65] (Fig. 8, *a*). In [17] the absorption was controlled by the subsequent transition $6^3P_2 \rightarrow 7^3S_1$, and the experimental results were compared with calculations

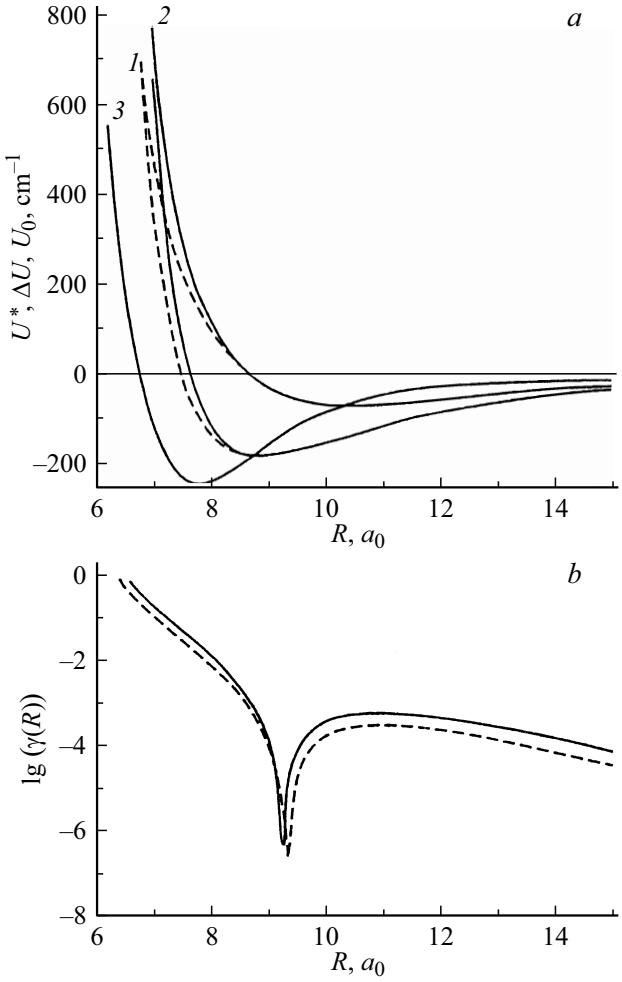

Figure 9. (*a*) Hg-Xe interaction potentials: *1* — $U^*(c1(^3P_2)$, *2* — difference potential ΔU, *3* — ground state potential U_0;(*b*) radiation width related to the width of the atomic state $Xe(5p6s^3P_2)$. Solid and dashed lines correspond to two different sets of experimental data for radiating quasimolecular states [77].

in the approach described in Sections 1.2, 1.3, using experimental data on $Hg(^3P_1 - {}^1S_0)$–Ar transitions [76] (Fig. 8, *b*). Both calculations and experimental data not only for Hg–Ar, but also for Hg–Kr, Xe [77] confirm the main conclusions obtained from the consideration of Hg–He, Ne quasimolecules. Quasimolecular transitions during pair collisions form a satellite located in the short-wavelength region with respect to the atomic transition $Hg(^3P_2 - {}^1S_0)$, the position of the maximum of which shifts towards higher frequencies with temperature rise. The difference in the positions of the absorption and emission maximums relates to the nature of the nature of distance dependence of the terms of the ground and excited states and the radiation width (Fig. 9). Since these dependences were constructed in [16,52] on the basis of various experimental studies, Fig. 9 also allows one to judge about „stability" of the semi-empirical method for determining terms and widths.

Quasimolecules with atoms of heavy inert gases X = Ar, Kr, Xe are characterized by the presence of a

minimum in the term $c1(^3P_2)$ at $R \sim 10a_0$ with depth $D_e \sim kT$ (Table 6). Therefore, in contrast to $X = \mathrm{He}, \mathrm{Ne}$, the question arises of how transitions involving vibrational states ν, ν' of the excited and ground states affect the shape of the spectrum. Considering such states instead of (1), one should write the processes of emission and absorption under the conditions of gas cell as

$$M(^3P_2) + \mathrm{Rg}, M\mathrm{Rg}(c1^1P_2, \nu) \leftrightarrow M(^1S_0) + \mathrm{Rg} + \hbar\omega, M\mathrm{Rg}(X^1S_0, \nu) + \hbar\omega. \quad (30)$$

In he approximation of paired collisions and for classical trajectories this question is solved when calculating the shape of the spectrum based on formula (28) by limiting the upper boundary of the region of integration with respect to the impact parameters by the value of the orbiting parameter [53,55]. For experiments under gas cell conditions, the contour, obtained in this way, in radiation corresponds to the low density limit. In the high-density limit, conversion with increasing of the inert gas density and three-particle collisions lead to a thermodynamically equilibrium population of vibrational states in $c1(^3P_2)$ term. So in this limit, when

$$\kappa\tau_p[N] > 1 \quad (31)$$

(κ — rate constant of vibrational relaxation, τ_p — characteristic radiative lifetime of the state, $[N]$ — density of atoms), the formula again turns out to be valid (28) [54]. As shown in [46], the orbiting leads to decreased fraction of transitions in radiation with a slight shift from the position of the forbidden atomic transition. The effect of orbiting on the shape of the radiation spectrum of Hg−Kr, Xe is considered in [77]. Apparently, the effect of orbiting on absorption was not considered, although in this case the effect should be more significant, considering the greater depth of the potential energy well in the ground state. The effect of deviation from thermodynamic equilibrium on the profile of spectral line wing was considered in [78]. As follows from the results of this paper, under the conditions of experiments in gas cell based on emission of vibrational states in the term $c1(^3P_2)$ we can assume that the excited molecules are in a thermodynamically equilibrium state.

As noted in Section 1.5, for Cd-Rg quasimolecules the presentation of $c1(^3P_2)$ state, which is not associated with nonadiabatic interaction with other states, is no longer justified. Therefore, in [54] the spectral profiles induced by $\mathrm{Cd}(5^3P_2)$ collisions with Ar, Kr atoms are calculated for $T = 300$ and 700 K. As in the case of Hg, the emission spectrum is a continuous band shifted to the short wavelength region compared to the position of the forbidden atomic line $\mathrm{Cd}(5^1S_0-5^3P_2)$. Since the depth of the potential energy well of the initial state is less than kT (Table 6), the band is formed mainly by transitions in two-particle collisions in the vicinity of the turning point in the classical motion of atoms, and the position of the radiation maximum depends weakly on temperature, its magnitude decreases with temperature rise. Absorption also forms a continuous band in the short-wavelength region, which leads to selective population of the 5^3P_2 state of atoms with a kinetic energy exceeding the thermal energy.

1.8. Effect of nonadiabatic transitions on the shape of the spectrum of quasimolecules

In the previous Section the spectra were calculated using the quasistatic approximation formulas (28), (29), which are very clear — they are simply the probabilities of emission/absorption of photon by pair of atoms at distance R. The derivation of such formulas is based on the estimation of the integral (27) by the saddle point method. The disadvantages of the formulas are related to the fact that they do not consider the possibility of the extremum existence in the difference potential $\Delta U(t)$, which, for example, necessarily takes place in the vicinity of the turning point of the classical trajectory and leads to the appearance of „rainbow“ [79]. In the paper [80] a formula was obtained that considers interference effects in the presence of extremum in the difference potential, if the extremum is located far from the turning point of the classical trajectory of atoms. Using the quadratic approximation $\Delta U(t)$ in the vicinity of the Condon point, we can express in [79,80] the transition amplitude in terms of the Airy function. The disadvantage of the used approximation is obvious; it is valid for transitions in the vicinity of the extremum only. A more general description based on the $\Delta U(t)$ approximation of the Morse functions and the exponential dependence of the radiation width is proposed in [81,82]. In this approximation the amplitude is expressed in terms of a parabolic cylinder function with a complex exponent, which made it possible to describe in a unified way the Lorentz line center, line wings, and also the satellite generated by the extremum of the difference potential [83]. The use of this formula led to good agreement with the experimental data on absorption for the asymptotically forbidden transition

$$\mathrm{Ca}(4s^2{}^1S_0) + \mathrm{He} + \hbar\omega \rightarrow \mathrm{Ca}(4s3d^1D_2) + \mathrm{He}$$

in [84]. Finally, in [85,86] a uniform quasiclassical description of the general case of a radiative transition between two exponential terms and a radiation width that depends exponentially on distance is obtained. The transition to quasiclassical theory made it possible, in particular, to describe the shape of the emission band [87] in the reaction

$$\mathrm{Ar}(3p^54s^3P_2) + \mathrm{He} \rightarrow \mathrm{Ar}(3p^6{}^1S_0) + \mathrm{He} + \hbar\omega$$

at collision energies $\sim 100\,\mathrm{cm}^{-1}$.

Another limitation of the quasistatic approximation used in Section 1.7 relates to the assumption that the state of $c1(^3P_2)$ quasimolecule is sufficiently isolated so that nonadiabatic transitions to other states can be neglected, and this is well justified for the experimental data obtained in gas cells. But when passing, for example, to quasimolecules, including atoms of the main subgroup II the group of

elements of the Periodic Table, especially light alkaline earth elements, then such assumption will no longer be valid. Indeed, for example, the splitting $\Delta\varepsilon(^3P_2{-}^3P_1) = 106$ (Ca), 41 (Mg) $\text{cm}^{-1} \leq kT$, which should be considered when calculating the spectral profiles.

Further, when analyzing the process, it should be considered that radiative transitions occur at all interatomic distances at which the dipole moment is nonzero, while the nonadiabatic transition is localized in the vicinity of some R_0, the center of the limited transition region. Before reaching this region during the collision and after it, the system develops adiabatically, so that the spectrum can be described on the basis of formula (27). Of course, the distance dependences of both terms and dipole moments in these two regions will be different. Another important difference between the radiative transitions of the outer shells of atom — they are proportional to α^3, and can be considered in the framework of perturbation theory. Thus, the effect of nonadiabaticity on the shape of the spectrum can be considered in the following way — first, the problem of nonadiabatic transitions is solved, and then the spectrum is calculated with the obtained wave functions, which depend on R. The theory of non-adiabatic transitions in pair collisions of atoms was developed in sufficient details [88]. The only complication in calculating the shape of the spectrum is that in contrast to the collision theory, it is now necessary to know the corresponding wave function for all R, but not only in the asymptotic regions of large and small R.

As can be seen from Fig. 2, 4, that the terms of $nsnp$ configuration are characterized by a relatively weak dependence on distance at large R (the terms are almost horizontal) and a fast rearrangement in the range of averages $\sim (7{-}8)a_0$, i. e. situation qualitatively corresponding to Demkov model of nonadiabatic transitions [89]. Within this model, the band profile is determined by two parameters [90]:

$$\xi^* = \frac{\pi\Delta\varepsilon}{2\alpha\sqrt{\frac{2kT}{\mu}}}, \quad \Omega = \frac{2(\omega - \varepsilon_0)}{\Delta\varepsilon}. \tag{32}$$

The first of them is the Massey parameter (μ is the reduced mass of colliding atoms), which determines the probability of transition between states, and the second is the optical transition energy in units of $\Delta\varepsilon$ — splittings of atomic terms $^3P_{2,1}$, so energies of atomic levels in this scale are $\Omega = \pm 1$. Figure 10 shows the emission band profile for the case under discussion, i.e., it is assumed that two states interact, radiating and metastable, and initially before the collision only the metastable state is populated. The spectral profile consists of two contours. This is Lorentz contour with a center located at the place of the allowed transition $\Omega = -1$, and its intensity is determined by the probability of a nonadiabatic transition from the metastable to the radiating state. The second contour, a quasimolecular one, which can be called a satellite, is formed by radiative transitions at $R < R_0$ and $\omega \sim 1$ from a state that was metastable at large R, but the interaction in the region of small distances

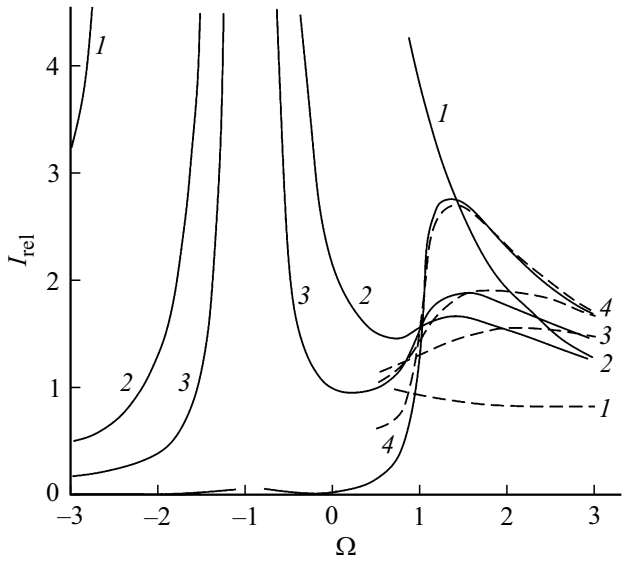

Figure 10. Collisionally induced spectrum averaged over the impact parameters and the Maxwell velocity distribution in the case of the initially populated state $^3P_2$ ($\Omega = 1$) [{] 90} for different values of the Massey parameter ξ^*. Solid lines — calculation within the framework of the Demkov model, dashed lines — calculation of the spectrum within the framework of the adiabatic approximation based on the formula (27): $\xi^* = 0.1$ (*1*), 0.5 (*2*), 1 (*3*), 5 (*4*).

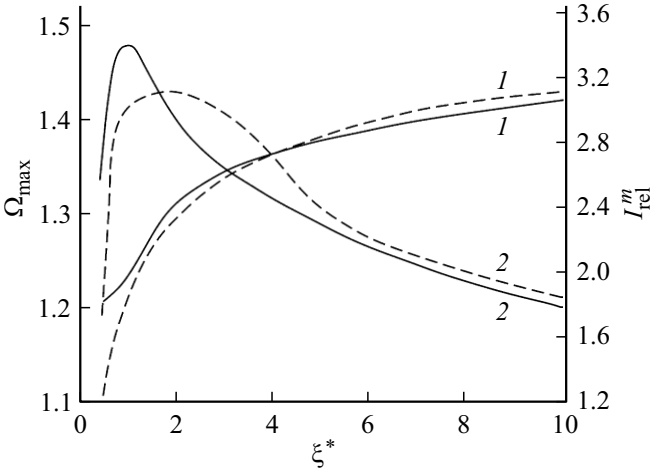

Figure 11. The intensity of the collisionally induced maximum of the satellite (*1*) and its position (*2*) depending on the Massey parameter ξ^* [90]. Solid curves — calculation within framework of the Demkov model, dashed curves — calculation in the framework of the adiabatic approximation based on formula (27).

led to partial transfer of the dipole moment of the radiating state. In the framework of the Demkov model for the interaction $V = V_0 \exp(-\alpha R)$, such a rearrangement of the radiation width is described by the formula

$$\Gamma_{qm}(R) = \Gamma_{at} \sin^2\theta(R), \;\; \theta(R) = \frac{1}{2}\,\text{arctg}\left(\frac{V_0}{\Delta\varepsilon}e^{-\alpha R}\right) \tag{33}$$

from paper [90], $\Gamma_{at,qm}$ are radiation widths of atomic diabatic and quasimolecular adiabatic states.

According to the basic idea of the theory of nonadiabatic transitions, collisions with $\xi^* \geq 1$ correspond to the adiabatic development of the system, so the spectral profiles under such conditions should be described by formulas (28), (29). Divergent adiabatic terms should be used as the excited state term in these formulas, and the adiabatic width should be used as the radiation width (Fig. 12, *b*, dashed curve). The dependence of the satellite intensity maximum and the position of its center Ω on ξ^* can be traced quantitatively in Fig. 11. It can be seen that for $\xi^* > 1$ the satellite profile is satisfactorily described by the formulas of the quasistatic approximation (27)–(29). Since, in the general case the satellite is formed during collision of atoms, in [90] it is called dynamic, in contrast to satellites in the line wings, which are associated with features, for example, extrema, depending on the terms U^*, U_0 from R.

Let's consider as an example the quasimolecules Ca, Mg–He. The terms and radiation width s of interest for radiative processes are calculated in the one-configuration approximation using the approach discussed in Sections 1.2, 1.3, and also in [18]. Comparison with multi-configuration calculations in [91] showed that in the cases under consideration one can limit to single-configuration calculations. The insignificance of the deviation from the Lande interval rule — 2.03 suggests that for the description of the collision process and the spectral profile by the interaction of only two nearest diabatic states $\varphi_{2,3}$ (Table 1) with the momentum projection $\Omega = 1$. Since the diabatic terms are parallel, the process of states interaction can be described in terms of Demkov model [90]. In Fig. 12 from the paper [92] the dashed curve marks the results of calculations of terms and radiation widths in the two-level approximation in the accepted model. As can be concluded from Fig. 12, for $R > 6.5a_0$ the use of the Demkov model is quite justified, and the quasistatic approximation is inapplicable, since $\xi^* = 0.8$ (Ca) and $\xi^* = 0.22$ (Mg) for $T = 1000$ K.

Figure 13 shows the spectrum formed during $\mathrm{Ca}(4^3P_2) + \mathrm{He}$ collisions [92]. As a result of the collision, the allowed atomic transition 4^3P_1–4^1S_0 with a red wing appears. This wing is formed by transitions in the region $R < R_0 = 8.8a_0$, the intensity of which is proportional to the probability of nonadiabatic transition and depends on the frequency as $(\omega_0 - \omega)^{-1}$. The satellite is formed in the violet wing, the maximum of which, according to the calculation within the framework of the Demkov model, is shifted to the violet region by 21 cm^{-1} from the position of $\mathrm{Ca}(4^3P_2 atomic level)$. As follows from the discussion above, the reason for the maximum appearance is associated with a sharp increase from zero to $\sim \Gamma_{at}/2$ of the radiation width when passing through the region of diabatic (atomic) functions rearrangement into quasimolecular ones. The refined calculation, which takes into account the interaction with 4^1P_1 atomic state (solid curves in Fig. 12, *b*), increases the shift by another 75 cm^{-1}. The calculation of the spectral profile in the case of Mg–He quasimolecule basically reproduces the already described characteristics of the spectrum for the Ca–He case, however, the probability increasing of nonadibatic transition with the splitting of atomic levels decreasing leads to the fact that the dynamic satellite does not appear against the background of the violet wing.

It is important to note that the spectrum description for the values of the Massey parameter $\xi^* < 1$ is possible only considering the interaction of states, while the summation of the spectra calculated in the quasistatic approximation, the intensities of which are even „corrected" considering the probability of nonadiabatic transition, does not reproduce the shape of the resulting spectrum. Another feature — the shape of the spectrum depends on which atomic state was originally populated, 4^3P_1 or 4^3P_2 [90,92,93].

2. Quasimolecules $\mathbf{Rg}(np^5(n+1)s) - \mathbf{Rg}'(^1S_0)$

2.1. Introduction

Theoretical approaches related to the description of radiative transitions in asymmetric quasimolecules of inert gases, including such transitions that are forbidden in the limit of large interatomic distances, were already discussed in review papers [94,95] He–Ne quasimolecule in different electronic states, which is interesting for laser physics, is reviewed in [96]. Experimental results of radiative transitions in asymmetric quasimolecules are collected and commented on in the Gerasimov's review [97]. Therefore, below we consider individual works carried out after the publication of the cited reviews.

The choice of the electronic configuration indicated in the header is not accidental. As above, an essentially two-particle problem will be considered — one electron and one hole, i. e. still 4 atomic states, but in reversed order. (Of course, in the case of the configuration $\mathrm{Rg}(np^5n'l, l > 0)$, this analogy disappears.) The appearance of the state radiation width $\Omega = 1$ is also due to interaction of three states, the terms of which go into atomic $^3P_{2,1}$ and $^1P_1$ (or into $s_{5,4,2}$ in Paschen notations) for large R.

For *s*-electron in inert gas atom, the effective charge is ~ 1, and for *p*-electrons ~ 4 [58]. The small bond energy of the excited electron justifies the well-known analogy $\mathrm{Rg}(np^5(n+1)s)$ with alkali metal atom following $\mathrm{Rg}(^1S_0$ atom in the Periodic Table, and allows us to use reliably established terms of the alkali metal–inert gas atom quasimolecules in the semiempirical procedure for restoration of the terms of Section 2.5. It is also qualitatively clear that the effect of the exchange interaction of the ionic core with the buffer gas atom will be more significant than the exchange interaction involving excited electron.

2.2. Quasimolecules of light inert gases

The paper [98] presents the results of the first multi-configuration calculation (MRD-CI) of the excited states of

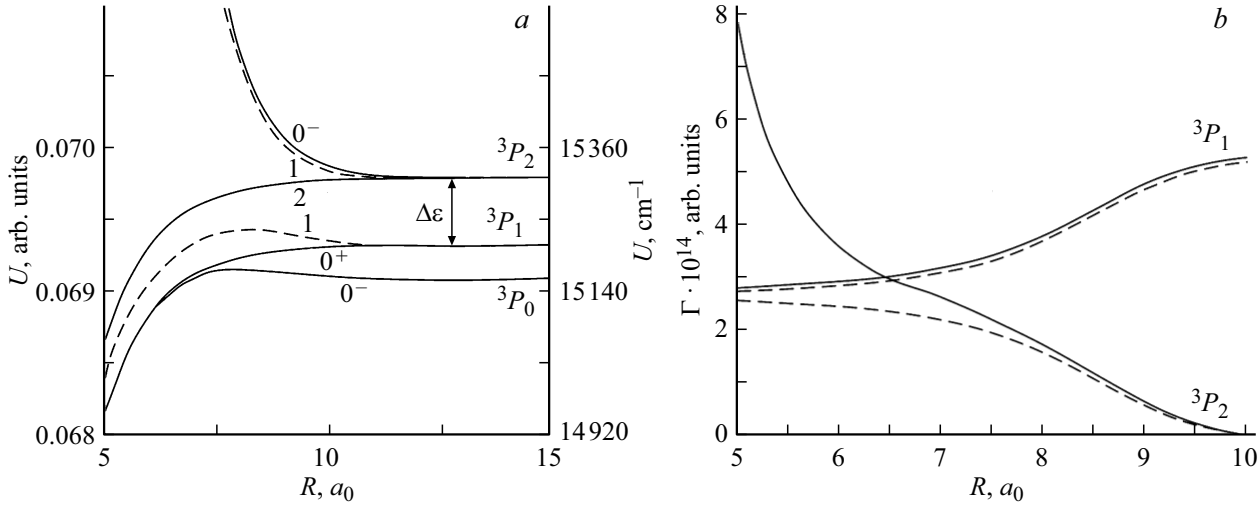

Figure 12. Quasimolecular terms (*a*) and widths (*b*) Ca($4s4p^3P_{j=0,1,2}$)−He. Solid curves — one-configuration calculation, dashed curves — approximation of two states [92].

Ne−He quasimolecule, which at large R correspond to the states Ne($2p^5ns$, $n'p$, $n''d$)−He($1s^2$), $n = 3, 4, 5$, $n' = 3, 4$, $n'' = 3$ and Ne($2p^6$)−He($1s2s^{1,3}S$). The calculations confirmed the correctness of the conclusion made in [99] for $n = 3$ — the region of strong bond of states $1(^3P_2)$ and $1(^3P_1)$ is not reached in thermal collisions, which makes it possible, in particular, to safely neglect the contribution of radiative quenching of the atomic state $^3P_2$ compared to nonadiabatic transition to the nearest state $^3P_1$. The calculations in [99] were carried out within the framework of the pseudopotential method and were essentially asymptotic, valid for $R > 5a_0$, while in [98] it was possible to move into $R > 2.5a_0$ region, where a potential energy well ($R \sim 3a_0$) with depth of about 500 cm^{-1} was found, exceeding the level energy $^3P_2$ to $\sim 500\,\text{cm}^{-1}$. Similar features were established in calculations involving the pseudopotential for terms generated by states with $n = 4.5$, which is related to the behavior of the s-function of an excited electron [96].

Calculation of terms and dipole moments of the lower excited configuration Ar($^3p^54s^{1,3}P$)−Ne using the MRD-CI method with relativistic core potentials (RECP) [100] allowed us to make an interesting comparison with the results of calculations using the pseudopotential [101] and the model potential [102]. For $1s_5$ state the calculation [100] showed the presence of potential energy well with a depth of 793 cm^{-1} at $R_m = 7.796a_0$, the calculation using the pseudopotential gave 40 cm^{-1}, $R_m = 8.5a_0$, and the calculation within the framework of the model potential did not reveal a minimum in the potential curve. Further, according to the results [100], the lifetime of $v = 0$ state in the well is 8.3 μs, while according to [101] the value is $1/\Gamma\lfloor 1(s_5), R \approx 7.3a_0\rfloor = 2$ ns. Apparently, it holds true to assume that most of the results obtained in the analytical approach using the pseudopotential and presented in [94–96] correctly reflect the essence of numerous processes involving excited atoms of inert gases, in particular, the

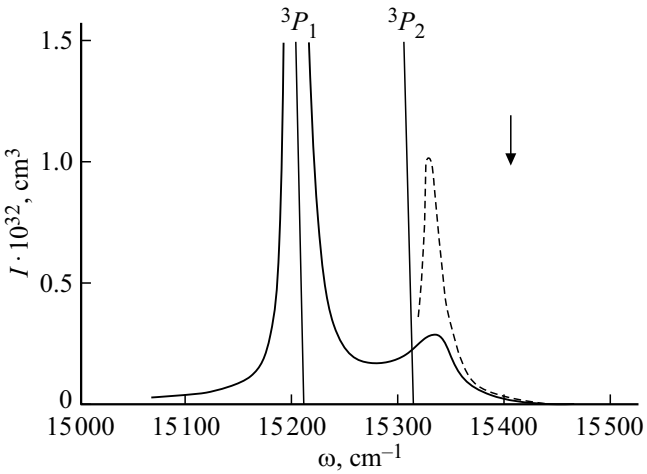

Figure 13. Ca-He quasimolecule. Spectral intensity vs. frequency [92]. Solid vertical lines mark the positions of atomic levels $^3P_{1,2}$. Dashed curve — quasimolecular transition ($\Omega = 1$, $4s4p^3P_2) \rightarrow (\Omega = 0^+, 4s\{2\}^1S_0)$ in the quasistatic approximation (28). The vertical arrow marks the shift of the maximum when the interaction with $^1P_1$ state is considered. Solid line — calculation within the framework of the Demkov model for the initial population of state $^3P_2$.

cause of the occurrence of the dipole moment of transition $1(^3P_2) \leftrightarrow 0^+(^1S_0)$. As for the reliable quantitative results for individual quasimolecules then the advantage of different options of *ab initio* calculations is indisputable.

2.3. Quasimolecules of heavy gases

The calculation of the terms of asymmetric quasimolecules formed by atoms of heavy inert gases in semiempirical approach similar to that described in Sections 1.2, 1.5 was already commented in detail in [95,94]. Table 10 shows the parameters of potential energy wells calculated in this

Table 10. Equilibrium internuclear distances and depths U_m of potential energy wells for $1(s_5)$ state of quasimolecules Xe*+Ar, Xe*+Kr and Kr*+Ar [103]

Parameter	Xe*+Ar	Xe*+Kr	Kr*+Ar
R_m, a_0	7.75	6.50	6.00
	7.75*	6.15*	6.05*
		5.89**	
U_m, cm^{-1}	438.9	1119	526.7
	307.3*	1119*	855.9*
		51**	

Note. * — experimental data [105], ** — calculation [104].

approach for some quasimolecules [103]. As can be seen, heavy quasimolecules are characterized by the presence of potential energy wells that are much larger than kT. In empirical approach, one can also calculate the widths of radiative transitions in the same way as described in Section 1.6. Here it is appropriate to refer to the remark at the end of the previous Section. In [104] the states $Xe(^3P_{1,2})-Kr$ are calculated in the *ab initio* approach, taking into account relativistic corrections and correlation electrons. Despite the coincidence of the structure of the terms and the position of the minima in the region of mean distances $R < 10a_0$, the values of the potential minima diverge (Table 10).

For quasimolecules of inert gases, the main difference from the results of Section 1 is that the determining interaction for the rearrangement of atomic diabatic functions will now be the distance-dependent splitting $V_{\Sigma,\Pi}$ of the terms of the molecular ionic core, which in the region of mean distances exceeds the interaction of an excited electron with the core. It is clear that the rearrangement affects both the formation of potential energy wells and the formation of the maximum of the dipole moment of the transition to the ground state, and, as a consequence, the lifetimes of vibrational states τ_v. Therefore, the value τ_v turns out to be very sensitive to the mutual arrangement of the potential energy well and the dipole moment dependence on R in this region.

In this paper [106] τ_v is calculated for excimers XeKr, XeAr, KrAr in the $1(^3P_2)$ state. For the considered pairs $R_m \sim (6-7)a_0$, the position of the radiation width maximum either coincides or is somewhat less than R_m, so the value of the integral $\tau_v^{-1} \sim \langle v|\Gamma|v\rangle$ is defined by a region R where the width decreases rapidly with increasing distance. As a result, τ_v increases with vibrational excitation increasing, while in the symmetric case Ar_2 [107] the dependence is opposite, since R_m for the symmetrical case is smaller and is located to the left of the position of the width maximum. Despite the fact that the lifetime is an integral characteristic, it turned out to be sensitive to the details of the interaction of atoms in the state $1(^3P_2)$ or $A1_u$.

In the paper [108], in particular, the effect of the difference of the potentials of the quasimolecular states and the radiation width on the averaged spectral profile was studied. The use of analytical approach made it possible to make the following observation. When analyzing the profiles of spectral lines by varying the dependences of the potentials and widths, good agreement is often achieved between the experimental and calculated data. But as it was demonstrated in [108], for asymptotically forbidden transitions, one must be careful with this approach. Different sets of terms for the ground and excited states can generate similar profiles, but in this case, due to the strong dependence of the radiation width on R, they give radiative quenching constants that differ by an order of magnitude. In such cases, analytical approaches to the determination of terms and widths can help to avoid errors in determining distance regions, transitions in which a decisive contribution to the integral and differential characteristics of radiative transitions are made.

2.4. Towards the full experience

Despite the fact that the use of experimental data in the foregoing was low and unsystematic, it is obvious that the discussed calculations were focused on experiments under gas cell conditions. Although the vast majority of experimental data on absorption or emission were obtained precisely under such conditions, double averaging (for example, over the impact parameters in the semiclassical approximation and the Maxwell distribution), which must be performed in calculations for subsequent comparison, masks the effect of the details of the behavior of the potential curves and dipole moments of the transition. Therefore, the study of differential cross sections for low-energy scattering with the recording of optical spectra and analysis of polarization could contribute to the understanding of radiative processes in the interaction of colliding atoms. A uniform quasiclassical approach can be useful here, it does not use known models of atomic collisions with a specific dependence of quasimolecular terms on distance and explicitly includes the dependence on the orbital angular momentum. The latter circumstance is important, since the orbital momentum increasing is accompanied by a qualitative change in the pattern of the optical spectrum formation.

Calculation examples are presented in papers [87], where the uniform semiclassical formula is used, in particular, to describe radiation at differential scattering $Ar(^3P_2) + He$ at collision energies 100, 200 and 1000 cm^{-1}, and [109], in which the first calculation was made for single-photon absorption in $He(1^1S) + Ne + \hbar\omega \rightarrow He(2^1S) + Ne$ with energy 219 cm^{-1}. In the last paper the dependence of the total and differential cross sections on the mutual orientation of the polarization vectors of the incident radiation and the initial relative velocity, as well as the detuning frequency on the atomic transition was established. It would be interesting to perform a similar calculation for the selective production of $Rg(^3P_2)$ atoms also.

3. Conclusion

The analytical approaches described above made it possible to discuss various radiative processes in pair collisions involving a rather wide range of atoms. Of course, such approaches cannot claim the accuracy achievable in *ab initio* approaches, but they provide the possibility of understanding the general regularities of various radiative processes during collisions. For applications, such approaches can also be useful, since they make it possible to relatively easily estimate the contributions of various processes to the population and decay of metastable states. Promising is the development of analytical approaches for the analysis of differential cross sections, in particular, with the participation of polarized atoms. Certain steps in this direction were already made in papers [110,111].

Acknowledgments

The author is especially grateful for the cooperation to his former graduate students and now colleagues, A.K. Belyaev, E.N. Bichutskaya, A.L. Zagrebin, N.A. Pavlovskaya, E.A. Chesnokov, and O.S. Alekseeva and M.G. Lednev also for their great help in preparing the paper.

Funding

The study has been funded by RFBR within the framework of the scientific project „Expansion“№ 20-12-50260/20.

Conflict of interest

The author declares that he has no conflict of interest.

References

[1] *Allard N., Kielkopf J.* // Rev. Mod. Phys. 1982. V. 54(4). P. 1103.
[2] *Garstang R.H.* // Atomic and Molecular Processes / Ed. by Bates D.R. Academic Press, 1962. 576 p. Translation: *Garstang R.* // Atomnye i molekulyarnye protsessy / Pod red. Biberman L.I., Fabrikant V.A. M.: Mir, 1964. P. 9.(in Russian).
[3] *Devdariani A.Z., Sebyakin Yu.N.* // ZhETF. 1989. V. 96. I. 6. P. 1997 (in Russian). *Devdariani A.Z., Sebyakin Yu.N.* // Sov. Phys. JETP. 1989. V. 96. N 7. P. 1127.
[4] *Dubov V.S., Nikonenko S.G.* // JETP. 1991. V. 72. N 3. P. 407.
[5] *Behmenburg W., Makonnen A., Kaiser A., Rebentrost F., Staemler V., Jungen M., Peach G., Devdariani A., Tserkovnyi S., Zagrebin A., Czuchaj E.* // J. Phys. B. 1996. V. 29. P. 3891.
[6] *Gallagher A.* // Atomic, Molecular, & Optical Physics / Ed. by Gordon W.F., Drake A. Springer, 2006. P. 220.
[7] *Allison D.C., Brown J.C., Dalgarno A.* // Proc. Phys. Soc. 1966. V. 89. P. 41.
[8] *Devdariani A., Leboucher-Dalimier E., Sauvan P., Angelo P.* // Phys. Rev. A. 2002. V. 66. P. 052703.
[9] *Devdariani A., Dalimier E., Sauvan P.* // Int. J. Spectr. 2010. V. 2010. Article ID 812471. Available at: http: // www.hindawi.com/journals/ijs/2010/812471.html. doi: 10.1155/2010/812471
[10] *Koperski J.* // Phys. Rep. 2002. V. 369. P. 177.
[11] *Devdariani A.Z., Zagrebin A.L.* // Opt. Spectrosc. 1985. V. 58. N 6. P. 752.
[12] *Nikitin E.E., Umanskii S.Ya.* Theory of Slow Atomic Collisions. Springer, 1984. doi: 10.1007/978-3-642-82045-8
[13] *Smirnov BM* Asimptoticheskie metody d teorii atomnykh stolknoveniy. 1973. 295 p. (in Russian).
[14] *Zagrebin A.L., Lednev M.G.* // Opt. i spektr. 1993. V. 74. I. 1. P. 24 (in Russian).
[15] *Zagrebin A.L., Lednev M.G.* // Opt. i spektr. 1985. V. 79. I. 6. P. 912 (in Russian).
[16] *Zagrebin A.L., Lednev M.G.* // Opt. i spektr. 1995. V. 78, № 2. P. 183 (in Russian).
[17] *Kurosawa T., Ohmory K., Chiba H., Okunishi M., Ueda K., Sato Y., Devdariani A.Z., Nikitin E.E.* // J. Chem. Phys. 1998. V. 108. N 19. P. 8101.
[18] *Zagrebin A.L., Lednev M.G.* // Opt. i spektr. 1992. V. 72. I. 3. P. 535 (in Russian).
[19] *Lurio A.* // Phys. Rev. 1965. V. 140. P. A1505.
[20] *Krykov N.A., Penkin N.P., Red'ko T.P.* // Opt. Spectrosc. 1981. V. 51. P. 756.
[21] *Czuchaj E., Krośnicki M., Stoll E.* // Chem. Phys. 1991. V. 263. P. 7.
[22] *Fermi E.* // Nuovo Cimento. 1934. V. 11. P. 157.
[23] *Zagrebin A.L., Lednev M.G.* // Opt. i spektr. 1993. V. 74. I. 1. P. 24 (in Russian).
[24] *Zagrebin A.L., Tserkovny S.I.* // Khim. fizika. 1990. V. 9, № 6. P. 727 (in Russian).
[25] *Ivanov G.K.* // Teor. eksp. khimiya. 1978. V. 14. № 5. P. 610; *Ivanov G.K.* // Theor. Exp. Chem. 1978. V. 14. N 5. P. 472.
[26] *Zagrebin A.L., Pavlovskaya N.A.* // Khim. fizika. 1988. V. 7. P. 435 (in Russian).
[27] *Zagrebin A.L., Tserkovny S.I.* // Khim. fizika. 1990. V. 9, № 6. P. 727 (in Russian).
[28] *Gruzdev P.F., Sherstyuk A.I.* // Opt. i spektr. 1976. V. 40. I. 4. P. 617 (in Russian).
[29] *Van Zee R.D., Blankespoor S.C., Zweier T.S.* // Chem. Phys. Lett. 1989. V. 158. P. 306.
[30] *Dashevskaya E.I., Devdariani A.Z., Zagrebin A.L.* // Khimiya plazmy. M.: Energoatomizdat. 1987. № 14. P. 127; (in Russian) *Dashevskaya E.I., Devdariani A.Z., Zagrebin A.L.* // Reviews of Plasma Chemistry. Kluwer. 1991. V. 1.
[31] *Devdariani A.Z., Zagrebin A.L., Lednev M.G.* // Khim. fizika. 1998. T. 17 № 6. P. 70 (in Russian). *Devdariani A.Z., Zagrebin A.L., Lednev M.G.* // Chem. Phys. Reports. 1998. V. 17. N 6. P. 1107.
[32] *Devdariani A.Z., Zagrebin A.L., Lednev M.G., Alekseev A.B., Liberman H.-P., Buenker R.J.* // Opt. i spektr. 2001. V. 91. P. 891 (in Russian). *Devdariani A.Z., Zagrebin A.L., Lednev M.G., Alekseyev A.B., Liebermann H.-P., Buenker R.J.* // Opt. Spectrosc. 2001. V. 91. N 6. P. 833.
[33] *Zagrebin A.L., Tserkovny S.I.* // Khim. fizika. 1990. V. 9, № 6. P. 727 (in Russian).
[34] *Zagrebin A.L., Tserkovny S.I.* // Khim. fizika. 1991. T. 10. № 5. P. 595 (in Russian).
[35] *Behmenburg W., Makkonen A., Kaiser A., Rebentrost F., Staemmler V., Jungen M, Peach G., Devdariani A.,*

Tserkovnyi S., Zagrebin A., Czuchaj E. // J. Phys. B. 1996. V. 29. P. 3891.
[36] *Buenker R.J., Peyerimhoff S.D.* // Theor. Chim. Acta. 1974. V. 35. P. 33.
[37] *Buenker R.J., Peyerimhoff S.D.* // Theor. Chim. Acta. 1975. V. 39. P. 17.
[38] *Buenker R.J., Peyerimhoff S.D., Butscher W.* // Mol. Phys. 1978. V. 35. P. 771.
[39] *Ermer W.C., Ross., Cristiansen P.A.* // Adv. Quant. Chem. 1988. V. 19. P. 139.
[40] *Alekseyev A.B., Libermann H.-P., Buenker R.J., Hirsh G., Li Y.* // J. Chem. Phys. 1994. V. 100. P. 8956.
[41] *Buenker R.J., Alekseyev A.B., Libermann H.-P., Zingott R., Hirsh G.* // J. Chem. Phys. 1998. V. 108. P. 3400.
[42] *Czuchaj E., Stoll H., Preuss H.* // J. Phys. B. 1987. V. 20. P. 1487.
[43] *Yamanauchi K., Isogai S., Okunishi M., Tsuchiya S.* // J. Chem. Phys. 1988. V. 88. P. 306.
[44] *Van Zee R.D., Blankespour S.C., Zwier T.S.* // Chem. Phys. Lett. 1989. V. 158. P. 306.
[45] *Duval M.-C., Jouvet C., Soep B.* // Chem. Phys. Lett. 1985. V. 119. P. 317.
[46] *Zagrebin A.L., Lednev M.G.* // Opt. i spektr. 1995. T. 79. № 6. P. 912 (in Russian).
[47] *Zagrebin A.L., Lednev M.G.* // Opt. i spektr. 1997. T. 83. № 2. P. 212 (in Russian). *Zagrebin A.L., Lednev M.G.* // Opt. Spectrosc. 1997. V. 83. N 2. P. 196.
[48] *Krykov N.A., Penkin N.A., Red'ko T.P.* // Opt. Spectrosc. 1989. V. 66. N 6. P. 1235.
[49] *Callear A.B, Du K.* // Chem. Phys. 1987. V. 113. N 1. P. 73.
[50] *Amano K., Ohmori K., Kurosawa T., Chiba H., Okunishi M., Ueda K., Sato Y., Devdariani A.Z., Nikitin E.E.* // J. Chem. Phys. 1998. V. 108. N 19. P. 8110.
[51] *Alekseeva O.S., Devdariani A.Z., Lednev M.G, Zagrebin A.L.* // Chem. Phys. Lett. 2013. V. 572. P. 141.
[52] *Zagrebin A.L., Lednev M.G.* // Opt. i spektr. 1995. T. 78. № 5. P. 758 (in Russian).
[53] *Ostroukhova I.I., Smirnov B.M., Shlyapnikov T.V.* // ZhETF. 1977. T. 73. № 1. P. 166 (in Russian).
[54] *Belyaev A.K., Devdariani A.Z., Sebyakin Yu.N.* // Opt. i spektr. 1985. V. 59. I. 3. P. 505 (in Russian).
[55] *Devdariani A.Z., Sebyakin Yu.N.* // ZhPS. 1985. V. 42, № 1. P. 29 (in Russian). *Devdariani A.Z., Sebyakin Y.N.* // J. Appl. Spectr. 1985. V. 42. N 1. P. 22.
[56] *Alekseeva O.S., Devdariani A.Z., Lednev M.G, Zagrebin A.L.* // J. Phys. Conf. Series. 2012. V. 397. P. 012031.
[57] *Ohmory K., Kurosawa T., Chiba H., Okunishi M., Sato Y., Devdariani A.Z., Nikitin E.E.* // Chem. Phys. Lett. 1999. V. 315. P. 411.
[58] *Sobelman II* Vvedenie v teoriyu atomnykh spektrov. M.: Nauka, 1977. 640 p. (in Russian). *Sobel'man I.I.* An Introduction to the Theory of Atomic Spectra. Elsevier, 1972. 608 p.
[59] *Devdariani A.Z., Kryukov N.A., Zagrebin A.L., Lednev M.G., Timofeev N.A.* // JQSRT. 2020. V. 248. P. 106951.
[60] *Devdariani A.Z., Klucharev A.N.* // Opt. Spectrosc. 1977. V. 42. N 6. P. 694.
[61] *Amusya M.Ya.* Atomny fotoeffekt. M.: Nauka, 1987. (in Russia)
[62] *Devdariani A., Kereselidze T.M., Noselidze I.L., Dalimier E., Sauvan P., Angelo P., Schott R.* // Phys. Rev. A. 2005. V. 71. N 2. P. 022512.
[63] *Alekseeva O.S., Devdariani A.Z., Zagrebin A.L., Lednev M.G.* // Khim. fizika. 2011. V. 30, № 11. P. 73 (in Russian). Rus. J. Phys. Chem. B. 2011. V. 5. N 6. P. 946.
[64] *Alekseeva O.S., Devdariani A.Z., Lednev M.G., Zagrebin A.L.* // Khim. fizika. V. 34. № 8. P. 9 (in Russian). Rus. J. Phys. Chem. B. 2015. V. 9. N 4. P. 515.
[65] *Yamanouchi K., Isogai S., Okunishi M., Tsuchiya S.* // J. Chem. Phys. 1988. V. 88. N 1. P. 205.
[66] *Koperski J., Łukomski M., Czajkowski M.* // Spectrochim. Acta. A. 2002. V. 58. P. 2709.
[67] *Radtsig A.A., Smirnov B.M.* Spravochnik po atomnoy i molekulyarnoy fizike. M.: Atomizdat, 1980. 240 p.; (in Russian) *Radzig A.A., Smirnov B.M.* Reference data on atoms, molecules and ions. Berlin: Springer-Verlag, 1985.
[68] *Kramers H.A., ter Haar D.* // Bull. Astr. Inst. Netherlands. 1946. V. 10. P. 137.
[69] *Bates D.R.* // Mon. Not. R. Astr. Soc. 1952. V. 112. P. 40.
[70] *Jablonski A.* // Proc. Int. Conf. on Opt. Pumping and Atomic Line Shapes. Warsaw, 1968. P. 323.
[71] *Szudy J., Baylis W.* // Phys. Rep. 1996. V. 266. P. 130.
[72] *Yakovlenko S.I.* Radiatsionno-stolknovitel'nye yavleniya. M.: Energoatomizdat, 1984. 209 p. (in Russian)
[73] *Devdariani A.Z.* // Opt. i spektr. 2015. T. 119. № 3. P. 356 (in Russian). *Devdariani A.Z.* // Opt. Spectrosc. 2015. V. 119. N 3. P. 333.
[74] *Zagrebin A.L., Lednev M.G.* // Pisma f ZhTF. 1989. V. 15, № 24. P. 11 (in Russian).
[75] *Zagrebin A.L., Lednev M.G.* // Opt. i spektr. 1998. V. 85, № 2. P. 200 (in Russian). *Zagrebin A.L., Lednev M.G.* // Opt. Spectrosc. 1998. T. 85. N 2. P. 181.
[76] *Sato Y., Nakamura T., Okunishi M, Ohmori K., Chiba H., Ueda K.* // Phys. Rev. A. 1996. V. 53. P. 867.
[77] *Zagrebin A.L., Lednev M.G.* // Opt. i spektr. 1999. V. 87. № 6. P. 893 (in Russian). *Zagrebin A.L., Lednev M.G.* // Opt. Spectrosc . 1999. V. 87. N 6. P. 812.
[78] *Rusov D.V., Sebyakin Yu.N.* // Opt. i spektr. 1999. V. 87, № 1. P. 22 (in Russian). *Rusov D.V., Sbyakin Yu.N.* // Opt. Spectrosc. 1999. V. 87. N 1. P. 16.
[79] *Devdariani A.Z., Ostrovskii V.N., Niehaus A.* // J. Phys. B. 1985. V. 18. P. L161.
[80] *Szudy J., Baylis W.E.* // JQSRT. 1975. V. 15. P. 641.
[81] *Devdariani A., Sauvan P., Leboucher-Dalimier E., Angelo P., Gauthier P.* // Rapport cienifique. 1996. Lab. L'Utilisation Laser Intenses Ecole Polytechnique NTIS: B97-170963. P. 115.
[82] *Devdariani A., Bichoutskaia E., Tchesnokov E., Bichoutskaia T., Crothers D.S.F., Leboucher-Dalimier E., Sauvan P., Angelo P.* // J. Phys. B. 2002. V. 35. P. 2469.
[83] *Devdariani A.Z.* // Opt. i spektr. 1999. V. 86. P. 954 (in Russian). *Devdariani A.Z.* // Opt. Spectrosc. 1999. V. 86. P. 853.
[84] *Bichoutskaia E., Devdariani A., Ohmori K., Misaki O., Ueda K., Sato Y.* // J. Phys. B. 2001. V. 34. P. 2301.
[85] *Devdariani A.Z.* // ZhETF. 1989. V. 96. P. 472 (in Russian). *Devdariani A.Z.* // J. Exp. Theor. Phys. 1989. V. 98. P. 486.
[86] *Devdariani A.Z., Chesnokov E.A.* // Khim. fizika. 1998. V. 17. № 6. P. 57 (in Russian). *Devdariani A.Z., Chesnokov E.A.* // Chem. Phys. Reports. 1998. V. 17. P. 10.
[87] *Devdariani A.Z., Zagrebin A.L., Rebentrost F., Tserkovny S.I. Chesnokov E.A.* // ZhETF. 2002. V. 122. № 3. P. 481 (in Russian).

[88] *Nikitin E.E, Smirnov B.M.* Medlennye atomnye stolknoveniya. M.: Energoatomizdat, 1990. 256 p. (in Russian)
[89] *Demkov Yu.N.* // ZhETF. 1963. V. 45. P. 195 (in Russian). *Demkov Yu.N.* // Sov. Phys. JETP. 1964. V. 18. P. 138.
[90] *Bichutskaya E.N., Devdariani A.Z., Sebyakin Yu.N.* // Opt. i spektr. 1998. V. 85, № 1. P. 11 (in Russian). *Bichoutskaya E.N., Devdariani A.Z., Sebyakin Yu.N.* // Opt. Spectrosc. 1999. V. 85. № 1. P. 7.
[91] *Zagrebin A.L., Tserkovnyi S.I.* // Opt. i spektr. 1993. V. 72. I. 2. P. 276 (in Russian).
[92] *Bichutskaya E.N., Devdariani A.Z., Zagrebin A.L., Sebyakin Yu.N.* // Opt. i spektr. 1999. V. 87, № 2. P. 213 (in Russian). *Bichoutskaia E.N., Devdarainai A.Z., Zagrebin A.L., Sebyakin Yu.N.* // Opt. Spectr. 1999. V. 87. N 2. P. 197.
[93] *Devdariani A.Z.* // Spectral Line Shapes. 1999. V. 10. 14th ICSLS ed. R.M. Herman: AIP Conf. Proc. 467. P. 325.
[94] *Devdariani A.Z., Zagrebin A.L., Blagoev K.B.* // Ann. Phys. Fr. 1989. V. 14. N 5. P. 467.
[95] *Devdariani A.Z., Zagrebin A.L.* // Plasma Chemistry / Pod. red. *Smirnov B.M.* Sb. statey. I. 15. M.: Energoatomizdat, 1989. P. 44 (in Russian).
[96] *Devdariani A.Z., Zagrebin A.L., Blagoev K.B.* // Ann. Phys. Fr. 1992. V. 17. N 5. P. 365.
[97] *Gerasimov G.N.* // UFN. 2004. V. 174. P. 155 (in Russian).
[98] *Buenker R.J., Liebermann H.-P., Devdariani A.Z.* // J. Phys. Chem. 2007. V. 111. N 7. P. 1307.
[99] *Devdariani A.Z., Zagrebin A.L.* // Opt. i spektr. 1985. V. 59. I. 2. P. 256 (in Russian). *Devdariani A.Z., Zagebin A.L.* // Opt. Spectrosc. 1985. V. 59. N 2. P. 155.
[100] *Petsalakis I.D., Buenker R.J., Lieberman H.-P., Alekseyev A.B., Devdariani A.Z., Theodorakopoulos G.* // J. Chem. Phys. 2000. V. 113. N 14. P. 5812.
[101] *Zagrebin A.L., Pavlovskaya N.A.* // Opt. i spektr. 1986. V. 62. I. 2. P. 264 (in Russian).
[102] *Spiegelmann F., Gadea F.X., Castex M.C.* // Chem. Phys. 1990. V. 145. P. 173.
[103] *Zagrebin A.L., Pavlovskaya N.A.* // Opt. i spektr. 1990. V. 69. I. 3. P. 534 (in Russian).
[104] *Jansik B., Schimmelpfennig B., Ågren H.* // Phys. Rev. A. 2003. V. 67. P. 042501.
[105] *Nowak J., Fricke J.* // J. Phys. B. 1985. V. 18. N 7. P. 1355.
[106] *Zagrebin A.L., Tserkovnyi S.I.* // Chem. Phys. Lett. 1995. V. 239. P. 136.
[107] *Madey A.A., Herman P.R., Stoicheff B.P.* // Phys. Rev. Lett. 1985. V. 57. P. 1574.
[108] *Devdariani A., Chesnokov E., Zagrebin A., Lednev M.G., Petsalakis I.D., Theodorakopoulos G., Liebermann H.-P., Buenker R.J.* // Chem. Phys. 2006. V. 330. P. 101.
[109] *Devdariani A., Chesnokov E., Rebentrost F.* // Chem. Phys. 2015. V. 462. P. 12.
[110] *Chesnokov E.A* // ZhETF. 2005. V. 128. № 5. P. 883 (in Russian).
[111] *Zagrebin A.L.* // ZhETF. 1990. V. 70. №1. P. 7 114 (in Russian). *Zagrebin A.L.* // Sov. Phys. JETP. 1990. V. 70. P. 64.